
# Supporting Information

for *Macromol. Chem. Phys.*, DOI: 10.1002/macp.202000373

# Building Bridges by Blending: Morphology and Mechanical Properties of Binary Tapered Diblock/Multiblock Copolymer Blends

Marvin Steube, Martina Plank, Markus Gallei, Holger Frey,* and George Floudas*

# Building Bridges by Blending: Morphology and Mechanical Properties of Binary Tapered Diblock/Multiblock Copolymer Blends

*Marvin Steube, Martina Plank, Markus Gallei, Holger Frey,* George Floudas**

Dr. Marvin Steube, Prof. Holger Frey
Department of Chemistry, Johannes Gutenberg Universität Mainz, 55099 Mainz, Germany
E-mail: hfrey@uni-mainz.de
ORCID H. Frey: 0000-0002-9916-3103

Martina Plank
Macromolecular Chemistry Department, Technische Universität Darmstadt, Alarich-Weiss Str. 4, 64287 Darmstadt, Germany

Prof. Markus Gallei
Chair in Polymer Chemistry, Saarland University, 66123 Saarbrücken, Germany
ORCID M. Gallei: 0000-0002-3740-5197

Prof. George Floudas
Department of Physics, University of Ioannina, P.O. Box 1186, 451 10 Ioannina, Greece
Max Planck Institute for Polymer Research, 55128 Mainz, Germany
E-mail: gfloudas@uoi.gr
ORCID G. Floudas: 0000-0003-4629-3817

**Keywords**: Polymer Blends, Tapered Block Copolymers, Gradient Copolymers, Miscibility, Phase Separation, Mechanical Properties, Tensile Tests

## Abstract

This work explores the scope and limitations of enhancing the poor mechanical properties of diblock copolymers by blending with tapered multiblock copolymers consisting of styrene and isoprene P(I-*co*-S)$_n$. Blending of different tapered diblock copolymers ($n$ = 1; 80 and 240 kg·mol$^{-1}$, 50 wt% polyisoprene (PI) units, lamellar morphologies) affords brittle materials with low elongation at break ($\varepsilon_{break} \approx$ 10 - 20%). In contrast, the analogous multiblock architectures ($n \geq 2$; 240-400 kg·mol$^{-1}$, 50 wt% PI-units, lamellar morphology) can bridge PS

domains, leading to resilient, highly stretchable materials ($\varepsilon_{break} \approx$ 670-800%). Based on the disparity of domain sizes an increasing degree of phase separation, from (i) miscible P(I-*co*-S)/P(I-*co*-S)$_n$ copolymer blends, to (ii) partially miscible and (iii) finally immiscible blends was studied. In the miscible binary P(I-*co*-S)/P(I-*co*-S)$_3$ blends the domain spacing, *d*, and the mechanical properties could be adjusted by introducing an amount of P(I-*co*-S)$_3$ hexablock copolymers with superior mechanical properties to the tapered diblock P(I-*co*-S). Fully miscible lamellar-forming binary blends maintain high elastic modulus, high strain at break and considerable toughness, continuously increasing with the P(I-*co*-S)$_3$ content, which reflects an increasing extent of domain bridging. Furthermore, the effect of miscibility on the mechanical properties was systematically studied for two diblock copolymers ($M_n$ = 80 and 240 kg·mol$^{-1}$, domain spacing of 38 nm and 77 nm, respectively), blended with a series of multiblock copolymers P(I-*co*-S)$_n$ ($n$ = 2 - 5; domain spacing of 42 to 20 nm) of similar molecular weight. Increasing disparity in the domain spacing, $\Delta d$, resulted in partially miscible and finally immiscible blends. Immiscibility caused lower elongation at break, albeit superior tensile properties compared to the pure tapered diblock copolymers ($\varepsilon_{break}\approx$20%) were maintained, surprisingly even for macrophase separated blends ($\varepsilon_{break} \approx$ 400%). The study shows that the addition of a minor fraction of multiblock copolymers to diblock copolymers is a versatile method towards improved mechanical properties, while retaining an ordered nanophase-separated morphology.

## 1. Introduction

Block copolymers can self-assemble into a variety of nanophase separated morphologies with applications ranging from nanolithographic processes to photonics, nanomedicine and nanoreactors.[1, 2] An application that has been in the focus of industrial[3, 4] as well as academic[1, 5] interest for more than 50 years, is their use as thermoplastic elastomers (TPEs), *i.e.* melt-processable, elastic materials. The most commonly used TPE architectures are based on ABA-type triblock copolymers that combine glassy, *i.e.* high glass transition temperature ($T_g$) end blocks with a rubbery, low $T_g$ midblock. In this case, phase-separated, vitrified domains act as thermoreversible crosslinks as well as a reinforcing filler in the rubbery matrix.[6] Thermoreversible crosslinking via high-$T_g$ blocks permits melt processing and also possesses potential for future recycling concepts.

Both step-growth[7] and chain-growth polymerization techniques[8] as well as their combinations[9] are used to generate TPEs, capitalizing on a broad range of different monomer combinations and polymer architectures. The living carbanionic polymerization of styrene with

1,3-dienes is known to be a versatile tool for the synthesis of controlled monomer sequences, high molecular weights and narrow dispersity.[10] For example, ABA triblock copolymers based on either polybutadiene (PB) or polyisoprene (PI) as low $T_g$ midblock with polystyrene (PS) A-blocks are probably the best investigated ABA-type block copolymer systems (A = PS; B= PB or PI).[11] A variety of different parameters, such as (i) the chosen monomer combination,[12] (ii) block sizes,[13, 14] (iii) block ratios,[15, 16] (iv) the extent of tapering[15–19] and (v) block sequences[20, 21, 18, 19, 22, 13] have been systematically explored. To further adjust or expand morphological and mechanical characteristics of well-understood polymer architectures, block copolymer blending represents an efficient and straightforward approach.[23]

Chemically joining two homopolymers to form a diblock copolymer increases their compatibility, and this is reflected in the reduction of the critical temperature for phase separation as compared to a homopolymer blend. For example, a binary mixture of A and B homopolymers phase separates at a critical value of the interaction parameter, $\chi$, such as $\chi \cdot N > 4$ (for $f$=0.5), as compared to a symmetric AB diblock copolymer with $N$ ($N$=$N_A$+$N_B$) monomer units that phase separates at a critical value of $\chi \cdot N$>10.5 (for $f$=0.5, according to the mean-field theory).[24] Thus, the formation of a diblock copolymer results in the reduction of the critical temperature for phase separation by a factor of 2.625. Since, in the simplest approximation, $\chi$ is inversely proportional to temperature, the higher critical value in the copolymers implies that diblock copolymers are more compatible than polymer blends. Compatibility can be further tuned by changing the molecular architecture, e.g. in tapered block copolymers or by blending different copolymers.

Binary diblock copolymer blends (AB+A'B') show miscibility depending on the ratio of molecular weights. Mixing of symmetric diblock copolymers with a small difference in their molecular weights (less than a factor of 2) was employed as a means of controlling the single order-to-disorder transition temperature and the (fluctuation-controlled) ordering kinetics.[25] However, blends of diblock copolymers with larger asymmetry in their molecular weights tend to phase separate. The miscibility of binary PI-*b*-PS diblock copolymer blends with different lamellar spacings was studied extensively by Hashimoto *et al*..[26, 27] Complete miscibility was found for block molecular weight ratios up to 1:5, whereas ratios of up to 10 resulted in partial miscibility and immiscibility.[26] In the partially miscible blends, it was shown that the copolymer with the lower molecular weight could hardly solubilize the copolymer with the higher molecular weight, e.g. the domain consisting of the lower molecular weight copolymer was nearly pure. These results were later confirmed by experimental results of Spontak[28] and predictions of Matsen, using a self-consistent field theory (SCFT).[29] In addition, blends of

diblock copolymers with antisymmetric compositions were able to form ordered LAM phases in their symmetric blends.[30]

To obtain tough and stretchable elastic materials, triblock copolymer architectures **(Figure 1)** consisting of a SIS or SBS block sequence, where I, B and S denote a PI, PB and PS blocks, respectively are highly established.[1] The vitrified high-$T_g$ end-block domains pin the long rubbery midblock at different domain boundaries (bridging conformation), which leads to excellent mechanical properties. The rheology of triblock copolymer containing blends with homopolymers and AB diblock structures (A+ABA; B+ABA; AB+ABA) has been investigated. Morton *et al.* evaluated the effect of synthetic imperfections (preliminary termination during anionic polymerization) on the resulting mechanical properties.[6] For this purpose, low contents of PS and PS-*b*-PI were blended with an SIS triblock copolymer. This pioneering work revealed profound effects on the tensile strength for even minor amounts of the diblock copolymer. Later, Cohen and Tschoegel established SI/SIS blends as a suitable model system to control the amount and length distribution of terminal, dangling PI chains in a rubbery network.[31] The combination of morphological investigations and theoretical predictions has proven to be a powerful tool in explaining the rheological features in terms of looping and bridging fractions.[32]

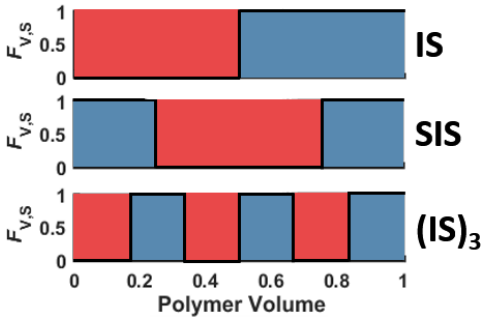


**Figure 1.** Monomer sequences of multiblock copolymers illustrated as volume based[18] copolymer composition profiles ($F_{V,S}$: instantaneous styrene volume incorporation).

In addition to triblock copolymers and their blends, multiblock copolymers with more than 3 blocks received considerable attention.[12, 33a, 20, 33b] Their repetitive block sequences enable bridging of two or more domains by a single polymer chain, giving rise to superior elastic moduli and increased stretchability of TPEs.[34–36, 20] The morphologies were investigated by Spontak *et al*. by mixing $(SI)_n$ tetra-, hexa- and octablock copolymers (*i.e.* (PS-*b*-PI)$_n$ with $n = 2 - 4$) with PS[37] and a tetrablock copolymer $(SI)_2$ with PI.[38] Blending experiments of an IS diblock copolymer with an $(IS)_4$ octablock copolymer revealed

macrophase separation already for a molecular weight ratio of 4:1.[39] The increased immiscibility of AB/$(AB)_n$ blends - relative to the diblock copolymer blends – were ascribed to the midblock conformations caused by the multiblock architecture.[52] Bates *et al*. presented the effective toughening of a fully hydrogenated SIS triblock copolymer by the addition of ≈ 15 wt% of a fully hydrogenated SISIS pentablock copolymer.[36]

Different from block copolymers, gradient copolymers show a comparably smooth block "transition" leading to an increased miscibility ($\chi_{eff} < \chi_{1,2}$).[40] Controlling $\chi_{eff}$ by the comonomer sequence is a versatile concept to decouple the phase segregation strength ($\chi_{eff} \cdot N$) from the molecular weight and obtain ordered nanodomains that are coupled via long chains.[15] As shown in our recent work, the consecutive multi-step copolymerization (alkyllithium initiation, hydrocarbon solvents) affords phase-separated tapered multiblock copolymers P(I-*co*-S)$_n$ with less synthetic effort compared to their sequential block analogues ((IS)$_n$ = (PI-*b*-PS)$_n$).[18] Their smooth block "transition" (*i.e.* $\chi_{eff} < \chi_{SI}$) lowers the order-disorder transition ($T_{ODT}$) in comparison to "non-tapered" block copolymers of the same composition. Consequently, the $T_{ODT}$ is located in a range typically used for high-speed processing of the polymer melt (e.g. $T_{ODT}$ ≈ 185 °C for P(I-*co*-S)$_3$ with $M_{n,total}$ ≈ 240 kg·mol$^{-1}$).[18] The industrial relevance of these structures and their miscible blends was demonstrated by Knoll *et al*. who studied binary homo- and triblock copolymer blends with tapered multiblock star copolymer architectures (e.g. trademark Styrolux).[41, 42, 3]

Herein we systematically explore the possibility of enhancing the poor tensile properties of tapered diblock copolymers based on polystyrene and polyisoprene by blending with a series of the respective tapered multiblock copolymers. To this end, different series of binary tapered diblock/multiblock copolymer blends (*i.e.* P(I-*co*-S)/P(I-*co*-S)$_n$ blends with $n$ = 2-5) were prepared. Their morphology was studied both by small-angle X-ray scattering (SAXS) and transmission electron microscopy (TEM). The mechanical properties of all blends were investigated by tensile testing. The study is organized as a function of increasing degree of phase separation, from miscible P(I-*co*-S)/P(I-*co*-S)$_n$ copolymer blends (Scheme 1, left part), to partially miscible and finally to immiscible blends (Scheme 1, right part). We correlate the distinct morphological changes in the blends with the pertinent mechanical properties. The results show strongly enhanced mechanical properties (elastic response, toughness) by the blending a limited amount of a multiblock copolymer with diblock copolymers.

## 2. Results and Discussion

TPEs based on (tapered) multiblock copolymer architectures effectively bridge the glassy polystyrene domains in the phase separated bulk state. This enables mechanical properties exceeding those of the corresponding diblocks by far. Here we explore the possibilities and limitations of enhancing the poor tensile properties of tapered diblock copolymers by blending with a series of tapered multiblock copolymers. The work is organized as follows: In the first part, we quantify this "multiblock toughening effect", by employing a fully miscible blend composed of a tapered diblock copolymer P(I-*co*-S) blended with a tapered hexablock copolymer P(I-*co*-S)$_3$. For this purpose, a series of polymer blends was prepared by solution-blending, only differing in the P(I-*co*-S)$_3$ (Scheme 1) content, and their morphology was identified by SAXS and TEM (chapter 2.1, below). In the second part (chapter 2.2) we investigate the effect of increasing immiscibility on the mechanical properties (. To this end we employ P(I-*co*-S)/P(I-*co*-S)$_n$ ($n$ = 2-5) blends with increasing differences in the domain spacing, $\Delta d$, of the constituent copolymers ($\Delta d = d_{\text{P(I-}co\text{-S)}} - d_{\text{P(I-}co\text{-S)}_n}$ with values ranging from -4 nm to 57 nm). **Table 1** provides the molecular characteristics of all three series of blends investigated herein. For both blend systems (chapter 2.1.2 and 2.2.2) the mechanical properties were studied via tensile testing.

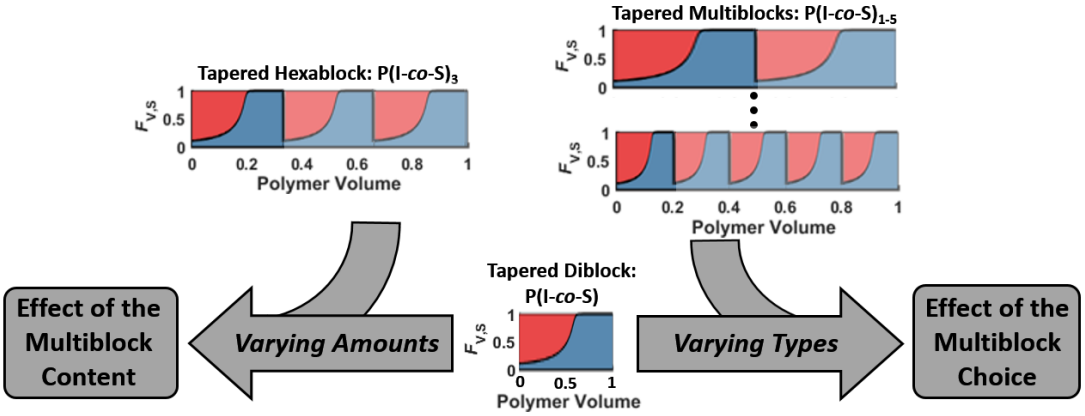


**Scheme 1.** Overview of the blending concepts applied in this work. Left: The P(I-*co*-S)$_3$ fraction was varied in a series of P(I-*co*-S)/P(I-*co*-S)$_3$ blends with similar $d$ ($\Delta d \approx 4$ nm). Right: The multiblock P(I-*co*-S)$_n$ was varied ($n$ = 2-5) in two series of P(I-*co*-S)/P(I-*co*-S)$_n$ blends. Following this principle, differences in domain sizes from $\Delta d$= -4 to 57 nm are covered for a constant P(I-*co*-S)$_n$ fraction (50 wt %).

**Table 1**. Molecular characteristics of the tapered block copolymers P(I-*co*-S)$_n$ ($n$ = 1-5) used for blending experiments. Each of the entries (1, 2 and 3) represents a series of blends. All tapered block copolymers exhibit 50 mol% PS and PI units, the latter being composed of 95 mol% 1,4-PI and 5 mol% 3,4-PI due to the polymer synthesis in cyclohexane.[18]

| Entry | $M_{n,\,target}$ a) [kg·mol$^{-1}$] | $M_{n,\,SEC}$ a,c) [kg·mol$^{-1}$] | Blend Composition | $M_{n,\,target}$ b) | $M_{n,\,SEC}$ b,c) [kg·mol$^{-1}$] | Changed Parameter |
|---|---|---|---|---|---|---|
| 1 | 80 | 92 | P(I-*co*-S)/ P(I-*co*-S)$_3$ | 400 | 512 | P(I-*co*-S)$_n$ Content: 0 - 100%$_w$ |
| 2.1 | 80 | 92 | P(I-*co*-S)/ P(I-*co*-S)$_2$ | 240 | 265 | $\Delta d$ = -4 to 18 nm |
| 2.2 | | | P(I-*co*-S)/ P(I-*co*-S)$_3$ | 240 | 268 | |
| 2.3 | | | P(I-*co*-S)/ P(I-*co*-S)$_4$ | 240 | 244 | |
| 2.4 | | | P(I-*co*-S)/ P(I-*co*-S)$_5$ | 240 | 248 | |
| 3.1 | 240 | 253 | P(I-*co*-S)/ P(I-*co*-S)$_2$ | 240 | 265 | $\Delta d$ = 35 to 57 nm |
| 3.2 | | | P(I-*co*-S)/ P(I-*co*-S)$_3$ | 240 | 268 | |
| 3.3 | | | P(I-*co*-S)/ P(I-*co*-S)$_4$ | 240 | 244 | |
| 3.4 | | | P(I-*co*-S)/ P(I-*co*-S)$_5$ | 240 | 248 | |

Molecular characteristics of a) P(I-*co*-S) and b) P(I-*co*-S)$_n$ with $n$ = 2-5. c) Deviations with respect to the targeted molecular weight are explained by an overestimation caused by the use of a PS standard. SEC diagrams were given in a previous work.[18]

## 2.1. Miscible Blends of Tapered Multiblock Copolymers

We first investigate the morphology and the associated mechanical properties in fully miscible blends with the lamellar (LAM) morphology.As will be shown below, a key factor controlling miscibility is the disparity in domain spacing (or equivalently, overall molecular weight) of the constituent copolymers. For this purpose, a series of blends was prepared consisting of the segregated tapered block copolymers P(I-*co*-S)$_n$ ($n$ =1 and 3), differing in their P(I-*co*-S)$_3$ content (**Table 1**, Entry 1). The copolymers used for these blends possess similar domain sizes (difference in domain spacings of the starting copolymers of $\Delta d$ = 4 nm).

### *2.1.1. Morphologies*

The SAXS patterns for the P(I-*co*-S)/P(I-*co*-S)$_3$ blends are shown in **Figure 2**. The scattering pattern of the tapered diblock copolymers display Bragg reflections at relative $q$ values of 1:2:3,

corresponding to a LAM morphology, possessing long-range order. Notice the suppressed intensity of the second Bragg peak relative to the odd-numbered reflections characteristic of PI and PS domains of equal volume. Moreover, the domain spacing of the individual copolymers P(I-*co*-S) and P(I-*co*-S)$_3$ scale as $d \sim N^{0.62}$,[18] (obtained from a series of molecular weights, details in [18]) revealing stretching of chains away from the ideal Gaussian configuration.

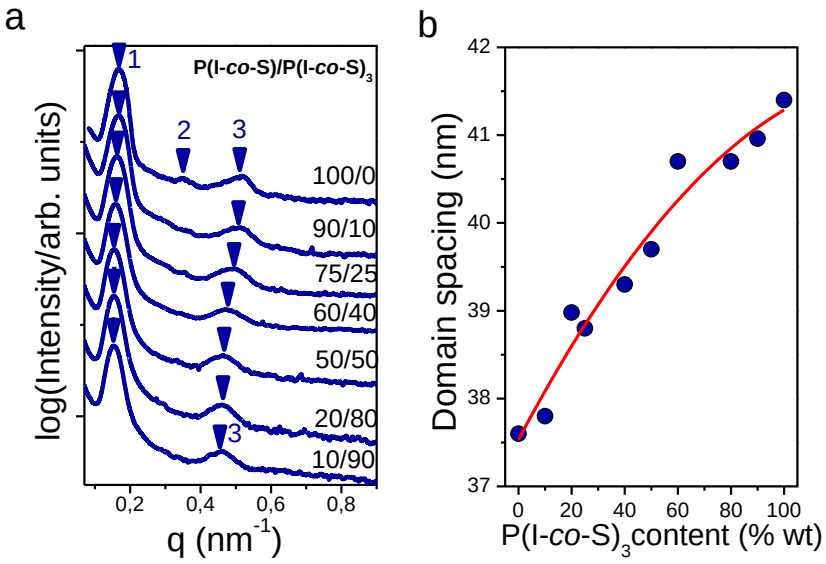


**Figure 2.** (a) SAXS patterns for the P(I-*co*-S)/P(I-*co*-S)$_3$ blends as a function of composition. The curves have been shifted vertically for clarity. Arrows give the positions of the Bragg peaks corresponding to a lamellar morphology. (b) Domain spacing as a function of blend composition. The line is a fit to a polynomial function and shown as a guide for the eye.

Blending of the tapered diblock with the P(I-*co*-S)$_3$ hexablock, having only slightly higher domain spacing, results in SAXS patterns that are not fundamentally different from the P(I-*co*-S) diblock copolymer. In general, the SAXS patterns of the blends **(Figure 2)** support the re-enforcement of the (similar) lamellar morphology by the P(I-*co*-S)$_3$. There are two findings that support this notion. First, odd numbered reflections still exhibit higher intensities excluding the possibility of incorporation of the P(I-*co*-S)$_3$ within a single nanodomain (the latter would change the X-ray contrast). Second, the (single) domain spacing follows a nearly linear correlation with composition, which underlines copolymer miscibility over the full composition range **(Figure 2b)**. The latter is obtained as $d = 2\pi/q^*$; $q^*$ is the modulus of the scattering vector corresponding to the first maximum (a closer inspection of the domain spacings of **Figure 2a** suggests a polynomial dependence as $d$ (in nm) $=37.6+5.72\times\varphi-1.96\times\varphi^2$, where $\varphi$ is the composition of P(I-*co*-S)$_3$ in the blends). These finding on the lamellar morphology are

confirmed by TEM on the same blends, now stained by $OsO_4$ (**Figure 3 and S1**). The only exception is the 60% P(I-*co*-S)$_3$ blend where a dual domain spacings with a minority component of larger spacing is evident in TEM.

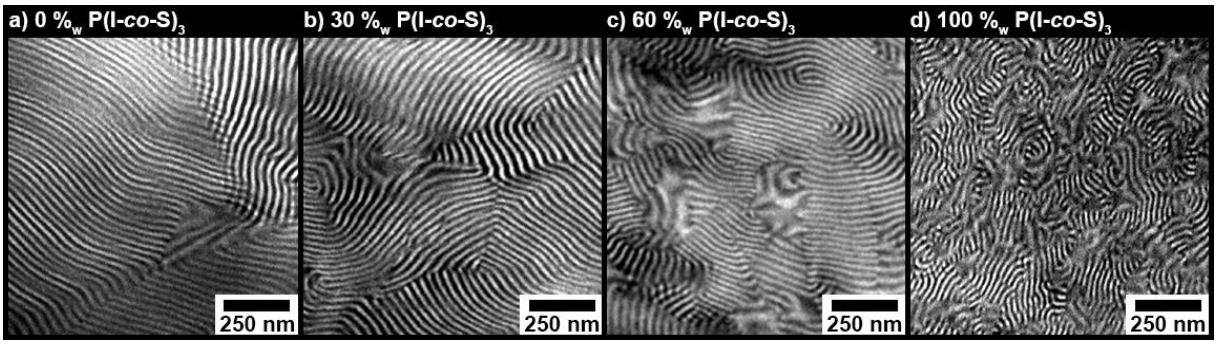


**Figure 3.** TEM measurements for P(I-*co*-S)/P(I-*co*-S)$_3$ blends with increasing content of P(I-*co*-S)$_3$. PI-rich phases are $OsO_4$-stained and appear electron opaque (dark).

Overall, the combined SAXS and TEM results confirm that the P(I-*co*-S)/P(I-*co*-S)$_3$ blends are fully miscible over the whole composition range. Given the disparate mechanical properties of the constituent copolymers (P(I-*co*-S) and P(I-*co*-S)$_3$ possess very different tensile properties), we explore in the following the effect of blending on the pertinent mechanical properties.

*2.1.2. Tensile Properties*

The tapered hexablock copolymer, P(I-*co*-S)$_3$, best combines structural integrity, with high mechanical toughness and a large strain at break.[18] Furthermore, the bridging capability of P(I-*co*-S)$_3$ over multiple glassy PS domains is expected to improve the mechanical properties of the blends. However, it is unknown to what extent a tapered diblock copolymer P(I-*co*-S), that is lacking mechanical re-enforcement can be incorporated into P(I-*co*-S)$_3$, maintaining toughness. To this end, films of P(I-*co*-S)/P(I-*co*-S)$_3$ with a varying P(I-*co*-S)$_3$ content were produced by solution-blending (with chloroform as a solvent) and subsequently exposed to uniaxial stress until rupture. **Figure 4a** visualizes the measured stress as a function of the strain $\sigma(\varepsilon)$ for a selection of representative blend samples (see **Figure S2** for other P(I-*co*-S)$_3$ contents). All blends exhibit similar characteristits, *i.e.* a regime of elastic response ($\varepsilon \approx 0\text{-}4\% < \varepsilon_{yield}$) followed by plastic flow ($\varepsilon_{yield} \approx 4\% < \varepsilon < \varepsilon_{break}$; $\varepsilon_{break}$ up to 800%), as anticipated due to their similar morphology. However, the blends containing 40% or more of the hexablock copolymer exhibit strain hardening beyond the yield point and show strongly enhanced toughness.

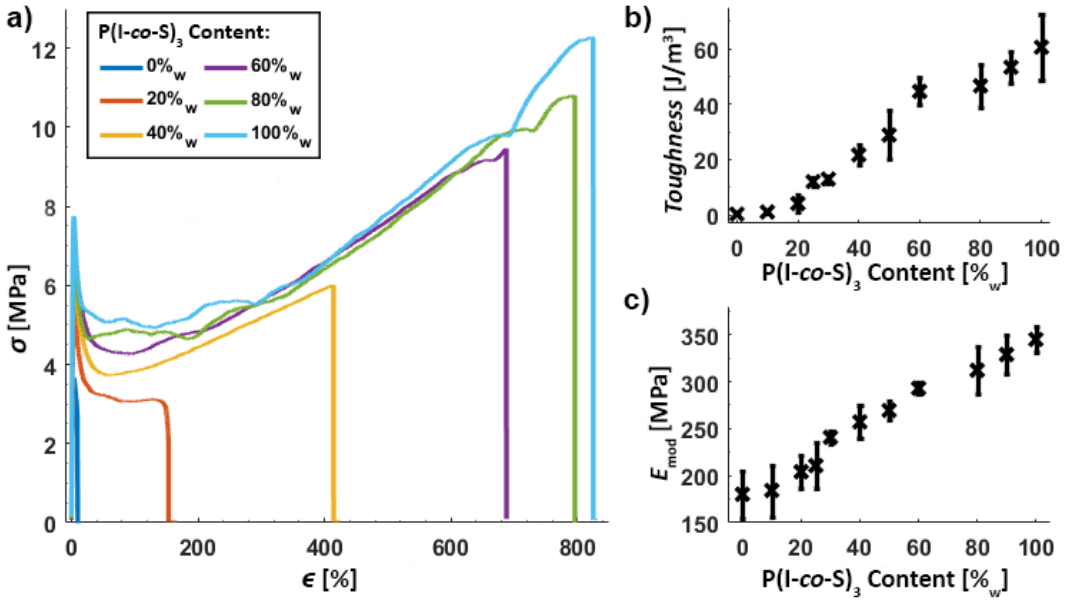


**Figure 4.** a) Representative stress-strain ($\sigma$-$\varepsilon$) diagrams, b) toughness and c) elastic moduli of miscible P(I-*co*-S)/P(I-*co*-S)$_3$ blends as a function of P(I-*co*-S)$_3$ content.

An increase of the P(I-*co*-S)$_3$ content in the blends results in a continuous increase of the strain at break from ≈ 10% to ≈ 800% **(Figure 4a and S2d; Table 2)**. In contrast, no significant changes are observed for the engineered stress $\sigma(\varepsilon)$. This is validated by toughness (*i.e.* integral of the tensile curve, **Figure S3)**, which shows a similar trend as the $\varepsilon_{break}$. Both the increase of $\varepsilon_{break}$ and of the toughness can be explained by the molecular architecture of the tapered hexablock copolymer. The covalent linkage of multiple blocks of P(I-*co*-S)$_3$ connects the vitrified high-$T_g$ microdomains by forming bridges in addition to entanglements, which imparts superior mechanical properties.[6, 43] Comparable observations were made by Lach *et al.* who studied toughening by blending a tapered SIS triblock copolymer with a tapered multiblock copolymer with a star topology.[41] However reported block copolymers possess different PS content, chain topologies and microdomain morphologies, precluding a direct comparison with the results in the current work (constant PS content, linear chain topology, lamellar phase state).

**Table 2.** Mechanical data of the miscible P(I-*co*-S)/P(I-*co*-S)$_3$ blending series (**Table 1**, Sample 1) determined via tensile testing. Uncertainties are given as a standard deviation ($\pm\sigma$ interval) from 8-15 independent drawing experiments on samples of the respective blend composition.

| P(I-*co*-S)$_3$ Content [wt %] | $\varepsilon_{yield}$ [%] | $\sigma_{yield}$ [MPa] | $E_{mod}$ [MPa] | $\varepsilon_{break}$ [%] | Toughness [J m$^{-3}$] |
|---|---|---|---|---|---|
| 0 | 3.7±0.2 | 4.2±0.7 | 180±25 | 10±5 | 0.33±0.15 |
| 10 | 3.9±0.2 | 4.4±0.9 | 180±27 | 41±19 | 1.1±0.3 |
| 20 | 3.9±0.1 | 5.2±0.5 | 200±17 | 120±89 | 4.2±3.1 |
| 25 | 3.9±0.1 | 5.3±1.0 | 210±24 | 340±56 | 12±2 |
| 30 | 3.9±0.1 | 6.2±0.2 | 240±6.2 | 320±26 | 13±1 |
| 40 | 3.8±0.2 | 6.6±0.8 | 260±18 | 450±86 | 22±4 |
| 50 | 3.7±0.1 | 6.8±0.3 | 270±9.7 | 540±153 | 29±9 |
| 60 | 3.7±0.1 | 7.4±0.2 | 290±5.6 | 700±55 | 45±5 |
| 80 | 3.7±0.1 | 7.5±0.6 | 300±22 | 720±92 | 47±8 |
| 90 | 3.6±0.2 | 8.0±0.7 | 330±20 | 750±63 | 53±6 |
| 100 | 3.7±0.1 | 8.5±0.4 | 340±14 | 800±96 | 61±12 |

At low strain ($\varepsilon < \varepsilon_{yield} \approx 4\%$; **Figure S2b,c and e**), sample deformation is fully reversible for all blends of this series and typically results in a linear increase of the stress $\sigma(\varepsilon)$ (**Figure S2b**). The slope of $\sigma(\varepsilon)$ (*i.e.* elastic or Young's modulus: $E_{mod} = \Delta\sigma/\Delta\varepsilon$; **Figure S3**) is visualized in **Figure 4c** as a function of P(I-*co*-S)$_3$ content. Increasing the latter leads to an increase of $E_{mod}$ up to the value of the P(I-*co*-S)$_3$ copolymer. The large value of P(I-*co*-S)$_3$ compared to P(I-*co*-S) is typical for multiblock copolymers as found in a series of $(IS)_n$ multiblock copolymers with increasing block number.[21, 20] A similar trend is observed for the yield point ($\varepsilon_{yield} \approx$ const.; $\sigma_{yield}$ increasing; for detailed discussion see **Figure S2**).[20] Both effects can be explained by an architecture-enhanced microstructural interconnectivity (*i.e.* increasing number of bridging conformations),[20] which enables the formation of midblocks pinned at both chain ends.[44]

The results presented here emphasize that in phase-matched, miscible blends of nano-phase separated tapered diblock copolymers, the domain spacing and the mechanical properties can be adjusted by introducing an amount of P(I-*co*-S)$_3$ multiblock copolymer. Although characteristic mechanical parameters, such as the toughness and strain at break show a gradual increase with the amount of added P(I-co-S)$_3$, the results demonstrate a significant effect of

domain bridging beyond 40% of added hexablock, leading to high toughness and a distinct strain hardening region.

### 2.2. Partially miscible or immiscible blends of tapered multiblock copolymers

In the ensuing part of the work, we increase the disparity, Δ*d*, of the domain sizes of the starting tapered copolymers and track the changes in morphology (miscibility) and tensile properties. Two series of P(I-*co*-S)/P(I-*co*-S)$_n$ blends were prepared (**Table 1**, Entries 2 and 3), only differing in the molecular weight of the tapered diblock copolymers P(I-*co*-S) (**Figure 5**, *d* = 38 nm and 77 nm, respectively). Tapered multiblock copolymers P(I-*co*-S)$_n$ with *n* = 2-5 and a constant molecular weight of 240 kg·mol$^{-1}$ were employed to systematically vary the difference in domain sizes, Δ*d*, within a given series (**Figure 5**; domain spacings varying from Δ*d* = -4 to 18 nm and 36 to 57 nm, in the two cases). Because of differences in the degree of segregation we discuss the two blend cases separately. The results of blends with 50 wt% of the multiblocks are summarized in **Table 3**.

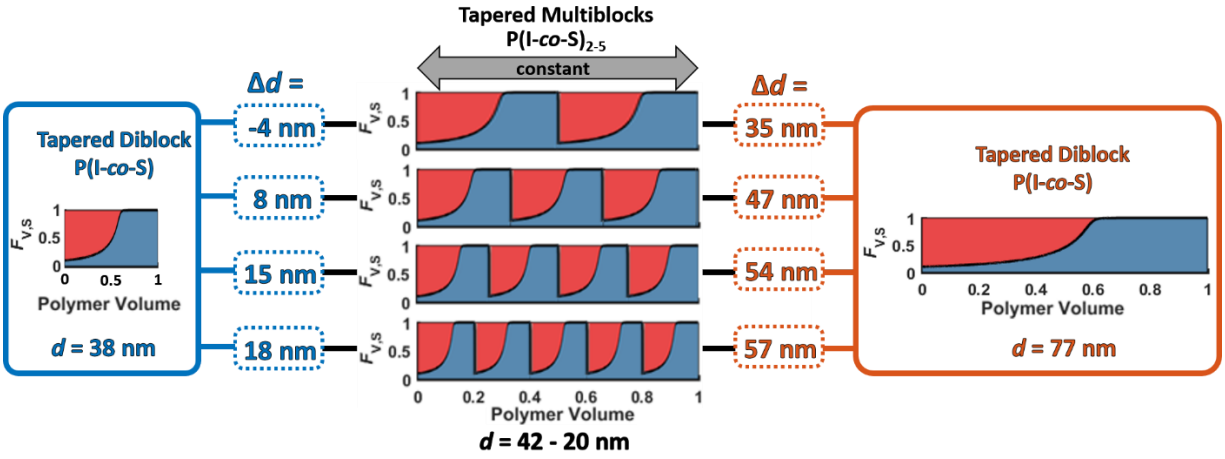


**Figure 5.** Overview of the prepared P(I-*co*-S)/P(I-*co*-S)$_n$ blends to study the effect of miscibility. Two series were prepared with systematic variation of Δ*d* by blending tapered diblock copolymers with similar series of tapered multiblock copolymers P(I-*co*-S)$_n$.

**Table 3.** Morphological and mechanical data of the P(I-*co*-S)/P(I-*co*-S)$_n$ blend series (50 wt% composition) determined via SAXS and tensile testing. Errors are given as the standard deviation (σ interval) from 8-15 independent drawing experiments. Molecular and mechanical characteristics of the starting (non-blended) copolymers are given in **Table 1 and S1**.

| Entry | *n* of P(I-*co*-S)$_n$ | $d_{P(I\text{-}co\text{-}S)}$ [nm] | $d_{P(I\text{-}co\text{-}S)n}$ [nm] | Δ*d* [nm] | *α* ratio[a)] | $d_{Blend}$ [nm] | Macrophase Separation | $\varepsilon_{break}$ [%] | Toughness [J·m$^{-3}$] |
|---|---|---|---|---|---|---|---|---|---|
| 1 | see Table 2 | | | | | | | | |
| 2.1 | 2 | 37.6 | 41.4 | -4 | 0.67 : 1 | 39.7 | no | 330±72 | 16±4.5 |
| 2.2 | 3 | | 29.8 | 8 | 1.0 : 1 | 32.1 | no | 500±85 | 28±7.1 |
| 2.3 | 4 | | 22.7 | 15 | 1.3 : 1 | 31.4 | no | 640±56 | 42±4.7 |
| 2.4 | 5 | | 19.9 | 18 | 1.7 : 1 | 31.8, 23.3 | partial | 610±54 | 41±5.4 |
| 3.1 | 2 | 76.6 | 41.4 | 35 | 2.0 : 1 | ~ 55 | partial | 450±37 | 31±3.3 |
| 3.2 | 3 | | 29.8 | 47 | 3.0 : 1 | 75, 30 | full | 440±29 | 23±1.2 |
| 3.3 | 4 | | 22.7 | 54 | 4.0 : 1 | 75, 23 | full | 390±24 | 21±2.7 |
| 3.4 | 5 | | 19.9 | 57 | 5.0 : 1 | 76, 20 | full | 370±22 | 20±1.6 |

a) Values correspond to the block molecular weight ratio $\alpha = M_{n,\,P(I-co-S)_n} / (n\ M_{n,\,P(I\text{-}co\text{-}S)})$. $M_n$: number averaged, targeted molecular weight (**Table 1**); *n*: number of repetitive tapered diblock segments in P(I-*co*-S)$_n$.

*2.2.1. Morphologies*

A series of symmetric blends (50 wt% diblock) was prepared, consisting of the segregated tapered block copolymers P(I-*co*-S) and P(I-*co*-S)$_n$ (*n* = 2-5) series with increasing disparity in domain sizes (Δ*d* = -4 to18 nm; **Figure 5** left part). The corresponding SAXS results are shown in **Figure 6**. As discussed in detail in a previous work,[18] domain sizes and LAM order decrease with increasing number of blocks (*i.e.* 2 *n*) in the P(I-*co*-S)$_n$ copolymers, when examined under constant molecular weight. On going from *n*=2 (the tetrablock) to *n*=5 (the decablock) the domain spacing is reduced from 41.4 nm to 19.9 nm and the disparity in domain spacings relative to the P(I-*co*-S) is enhanced from -4 nm to 18 nm. Moreover, increasing *n* progressively drives the copolymers from the ordered to the disordered state (*i.e.* in P(I-*co*-S)$_5$ with the broad structure factor due to correlation hole scattering). In the blends, miscibility and LAM order is preserved up to P(I-*co*-S)/P(I-*co*-S)$_4$, as confirmed by the single domain spacing – being intermediate to the constituent components - and the presence of higher order peaks. In the P(I-

*co*-S)/P(I-*co*-S)$_5$ case, however, where the disparity in domain spacings is maximized ($\Delta d$ = 18 nm), a bimodal domain spacing is observed by SAXS. From the peak positions relative to the starting copolymers the domain spacings correspond to a phase rich in P(I-*co*-S)$_5$ and another phase, where P(I-*co*-S) and P(I-*co*-S)$_5$ are mixed (**Table 3** and **Figure S4**). The effect of these distinct morphological changes on the mechanical properties will be discussed later.

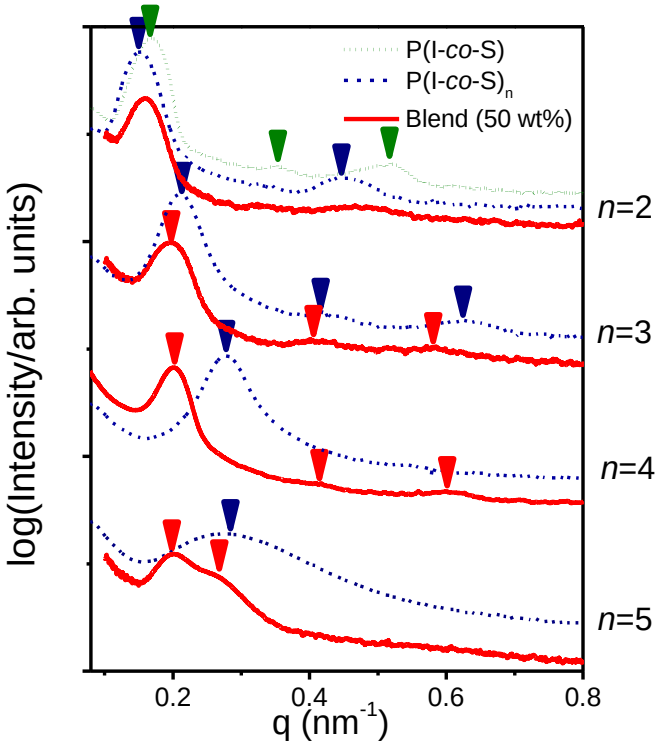


**Figure 6.** SAXS patterns for the P(I-*co*-S) (green dotted line), P(I-*co*-S)$_n$ copolymers ($n$=2-5; blue dashed line) and the corresponding binary symmetric (50 wt%) blends (red lines) (from entry **2** in Ta**ble 3**). The curves have been shifted vertically for clarity. Arrows give the positions of the Bragg peaks corresponding to a lamellar morphology.

In an effort to further increase blend immiscibility and to compare their tensile properties a third blend series was prepared (**Table 3**, entry 3), utilizing a tapered diblock copolymer with a larger domain spacing ($d$ = 76.6 nm; $M_{n,target}$ = 240 kg·mol$^{-1}$). Now the constituent blend components differ in their domain spacings by $\Delta d$ = 35 nm ($n$=2) to 57 nm ($n$=5). The SAXS patterns are visualized in **Figure 7**. As expected, they demonstrate macrophase separation. In P(I-*co*-S)/P(I-*co*-S)$_2$, however, a single but asymmetrically broadened peak is observed with a domain spacing characteristic of a mixed lamellar phase. The TEM study discussed below provides more insight regarding the asymmetric broadening

of the SAXS peak. In P(I-*co*-S)/P(I-*co*-S)$_3$ blends of this series there are two broad peaks with spacings of 47 nm and 43 nm, *i.e.*, intermediate to the constituent copolymers, suggesting partial phase separation into P(I-*co*-S)-rich and P(I-*co*-S)$_3$-rich domains. In P(I-*co*-S)/P(I-*co*-S)$_4$ blends, the two peaks have domain spacings of 75 nm and 23 nm that are nearly identical to the constituent copolymers, revealing complete phase separation, albeit in the absence of long range order. Lastly, in the P(I-*co*-S)/P(I-*co*-S)$_5$, there is full macrophase separation of the copolymer components (domains spacings of 76 nm and 20 nm, with perfect matching with the constituent copolymers ($\Delta d$ = 57 nm; **Table 3** and **Figure S4**). An interesting feature in the latter case is the second order reflection from the P(I-*co*-S) phase suggesting a well-ordered LAM phase within the P(I-*co*-S) domain, which will be correlated to TEM results below.

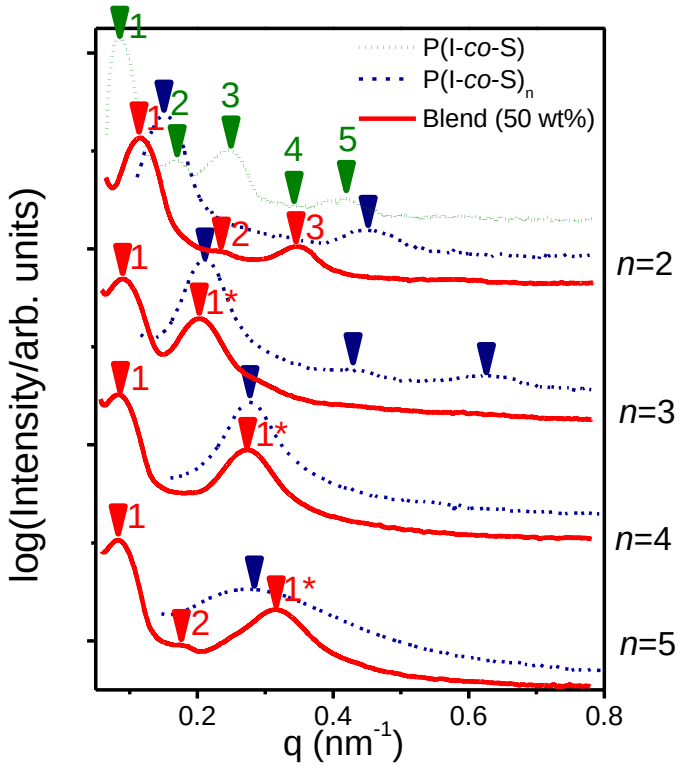


**Figure 7.** SAXS patterns for the P(I-*co*-S) (green dotted line), P(I-*co*-S)$_n$ copolymers ($n$=2-5; blue dashed line) and the corresponding binary symmetric (50 wt%) blends (red lines) (from entry 3 in **Table 3**). The curves have been shifted vertically for clarity. Arrows give the positions of the Bragg peaks corresponding to a lamellar morphology. Arrows with stars indicate the primary peak of the second phase.

The SAXS results can be compared with the results from the TEM investigation. **Figure 8a** (SAXS: $\Delta d$ = 35 nm; $n$ = 2; see also **Figure S5**) shows larger domains with a single domain spacing and some smaller domains of a larger spacing, in line with the asymmetric

SAXS peak. Lamellar grains with distinct spacings in the partially macrophase separated blend are highlighted in the insets. Increasing the difference in the domain spacing to $\Delta d$ = 57 nm (SAXS: $n$ = 5 in **Figure 8b**), leads to full macrophase separation in P(I-*co*-S)$_5$ and P(I-*co*-S) domains. While the diblock domains are well-ordered, the decablock domains are poorly ordered or even in the disordered state. TEM results are in excellent agreement with the results from the SAXS study for the P(I-*co*-S)/P(I-*co*-S)$_5$ blend with a highly ordered P(I-*co*-S) domain and a disordered P(I-*co*-S)$_5$ domains.

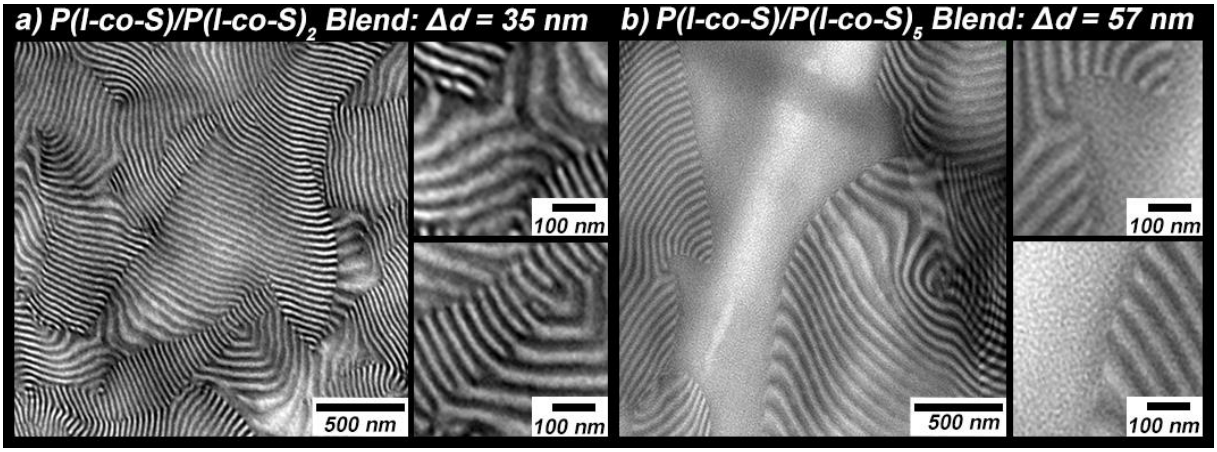


**Figure 8.** TEM measurements of a a) P(I-*co*-S)/P(I-*co*-S)$_2$ blend (**Table 1** entry 3.1) and a b) P(I-*co*-S)/P(I-*co*-S)$_5$ blend (**Table 1** entry 3.4). Insets visualize the interfaces of distinct grains. PI-rich phases are $OsO_4$-stained and appear electron opaque (dark).

The results from the P(I-co-S)/P(I-co-S)$_n$ blends should be compared with the corresponding blends composed from sequential multiblock copolymers (PI-*b*-PS)$_n$ with PI-*b*-PS investigated earlier by TEM. There, demixing was evident for a single (PI-*b*-PS)/(PI-*b*-PS)$_n$ blend (*cf.* **Figure 1**) with a block molecular weight ratio ($\alpha$) of 4 : 1,[39] which is lower than the 5.2 : 1 limit anticipated for binary PI-*b*-PS/PI-*b*-PS blends.[26–29] The increased immiscibility of the former blend was ascribed to the multiblock copolymer architecture, leading to bridged and looped midblocks, which reduce the lateral extension of chains. The series of blends investigated herein (see **Table 3**) (with α-ratios below 5.2 : 1) allow to track and to quantify this effect more precisely. In addition, they allow examining the effect of the different polymer topology (sequential vs. tapered) in driving macrophase separation. Our results reveal partial macrophase separation already for $\alpha$ = 1.7 : 1 and 2.0 : 1 (**Table 3**, entries 2.4 and 3.1) as well as full macrophase separation for $\alpha$ = 3.0 : 1, 4.0 : 1 and 5.0 : 1 (**Table 3**, entries 3.2-3.4) as observed, respectively, for the P(I-*co*-S)$_3$, P(I-*co*-S)$_4$ and P(I-*co*-S)$_5$ containing blends. Evidently, P(I-co-S)n copolymers reside at closer proximity to the interface than (PI-b-PS)n

due to the mismatch in periodicity and gradient composition. Localization of the tapered copolymer at the interface gives rise to defected sites that evedually lead to macrophase separation. This underlines the unique behavior of the (tapered) multiblock copolymers investigated in this work, which differs from the sequential block copolymers studied earlier. The effect of macrophase separation in the tensile properties is investigated next.

*2.2.2. Tensile Properties*

Immiscible P(I-*co*-S)/P(I-*co*-S)$_n$ blends separate into P(I-*co*-S)$_n$ rich and P(I-*co*-S) rich macrophases. Depending on the degree of mixing, as a consequence of the inhomogeneous nature of the samples certain macrodomains may have low P(I-*co*-S)$_n$ content (*i.e.* reduced number of bridges) that could lead to mechanical failure. Yet, it is unknown how the mechanical properties will depend on the content of such domains. To quantify the effect of immiscibility and the concomitant presence of grains with a variable composition and of the increased grain boundaries on the mechanical properties, we designed partially miscible and immiscible P(I-*co*-S)/P(I-*co*-S)$_n$ blends and investigated their mechanical properties by tensile testing.

Before we report on the blend series, we need to discuss the effect of increasing number of blocks on the tensile properties. Spontak *et al.* suggested that the mechanical properties of (PI-*b*-PS)$_n$ multiblock copolymers are improved with increasing number of blocks.[21, 20] This phenomenon was attributed to their capability of forming multiple bridged glassy styrenic domains, resulting in "stitched" domain boundaries.[18, 34, 45a, 21, 20, 45b] In the present P(I-*co*-S)$_n$ tapered copolymers investigated under a constant chain molecular weight by increasing the number of blocks, it was demonstrated that the mechanical properties (e.g. higher strain at break and elastic modulus) are a function of the number of blocks (*i.e.* **Figure 7**) and of domain mixing.[18] Increasing *n* beyond a certain number leads to a drop of mechanical properties (*cf.* **Figure 9** dashed lines and **Table S1**), explained by the disappearance of physical crosslinks caused by mixing of unlike domains as evidenced by SAXS.[18, 19]

**Figure 9** visualizes the toughness of P(I-*co*-S), P(I-*co*-S)$_n$ and the respective of P(I-*co*-S)/ P(I-*co*-S)$_n$ symmetric blends (50 wt%) as a function of the difference in domain spacing of the constituent copolymers, $\Delta d$. In the case of largely miscible P(I-*co*-S)/ P(I-*co*-S)$_n$ blends (**Table 1** Entry 2, **Figure 7**) where $\Delta d$ = -4 to 18 nm, the toughness (and the strain at break, **Figure S6a and S7a; Table 3**) follow the trend of the constituent P(I-*co*-S)$_n$ multiblock copolymers, albeit with lower values.

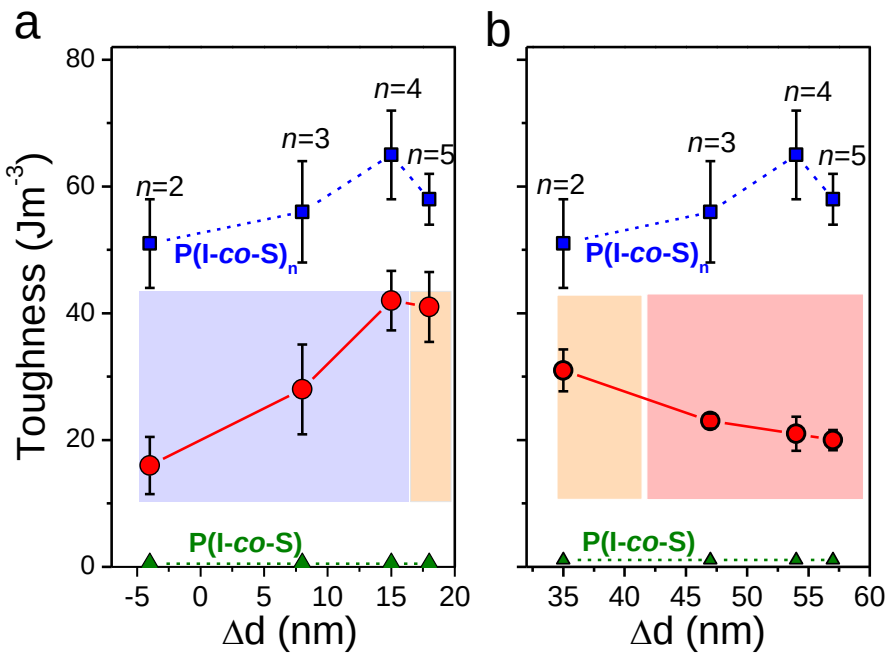


**Figure 9.** Toughness of P(I-*co*-S) (dashed green line), P(I-*co*-S)$_n$ (dashed blue line) and the respective blends (red line) as a function of Δ*d*. (a) Blending series with Δ*d* = -4 to 18 nm (red circles; **Table 1** Entry 2 and **Figure 6**). (b) Blending series with Δ*d* = 35-57 nm (red circles; **Table 1** Entry 3 and **Figure 7**). Lines are guide for the eye. Areas in blue, orange and red depict fully miscible, partially miscible and immiscible blends, respectively.

This situation is different for the P(I-*co*-S)/P(I-*co*-S)$_n$ symmetric blends (**Table 1**, Entry 3, **Figure 7**) with the higher molecular weight P(I-*co*-S) and the higher disparity in domain spacings of the P(I-*co*-S)$_n$ (Δ*d* = 36 – 57 nm), leading to full macrophase separation for Δ*d* = 47 nm, 54 nm and 57 nm (*i.e.* the P(I-*co*-S)$_n$ containing blends with *n* = 3-5 in **Figure 7** and 9b). Although this blend series contains the same P(I-*co*-S)$_n$ with the mechanically tough components as compared to the blends in **Figure 9a**, the trend in the mechanical behavior is remarkably different. Failure of these materials occurs already at rather low strain values (**Figure S6b** and **S7b**, **Table S1**), leading to a continuous decrease in toughness. This trend is tentatively explained by the formation of macrophase separated areas poor in P(I-*co*-S)$_n$ content (**Figure 7 and 8**). These areas possibly serve as local defects, facilitating crack initialization, growth and ultimate failure of the materials.[41, 46]

Despite the poorer mechanical properties of the macrophase separated blends than for the previously discussed series, it is remarkable that even a fully macrophase separated blend (**Table 3**, Entry 3.4) still exhibits a toughness of 20 J·m$^{-3}$, exceeding the value of the corresponding diblock by far (1.4 J·m$^{-3}$; **Table S1**, Entry 2). An interesting, and at first sight,

surprising exception is obtained by comparing the toughness of the P(I-*co*-S)/P(I-*co*-S)$_2$ blends (compare *n*=2 blends in **Figure 9a and b**). In this case, the partially macrophase separated blend (**Table 3,** Entry 3.1) exhibits an even larger toughness than the fully miscible analogue (**Table 3**, Entry 2.1; 31 J·m$^{-3}$ vs. 16 J·m$^{-3}$). A direct comparison of the $\sigma(\varepsilon)$ curves (**Figure S8**) reveals significant differences in the engineered stress. Although the P(I-*co*-S) is not capable of bridging vitrified PS domains, it affects the tensile strength in the P(I-*co*-S)/P(I-*co*-S)$_n$ blend at elongations far beyond $\varepsilon_{break}$ of the brittle P(I-*co*-S) material. This improved $\sigma(\varepsilon)$ is tentatively explained by the increased $T_{g,PS\text{-}rich}$ (100 °C vs. 80 °C)[18, 47] and $M_n$ (240 kg·mol$^{-1}$ vs. 80 kg·mol$^{-1}$) of P(I-*co*-S) in the partially macrophase separated blend (*cf.* **Table S1 and S2**). Increasing molecular weight further increases the number of entanglements and therefore imparts mechanical stability.

## 3. Conclusion

Diblock copolymers are known to show highly ordered domain structures, however they possess poor mechanical properties, since there is no bridging of nanodomains. We explored the possibilities and limitations of enhancing the poor tensile properties of a tapered diblock copolymer by blending with related, tapered multiblock copolymers in the lamellar phase. The study was carried out as a function of increasing degree of phase separation, from miscible P(I-*co*-S)/P(I-*co*-S)$_n$ copolymer blends, to partially miscible and finally to immiscible blends with large differences in their domain sizes.

In the fully miscible P(I-*co*-S)/P(I-*co*-S)$_n$ blends, *i.e.*, in blends of tapered diblock and structurally analogous multiblock copolymers having comparable domain spacings according to SAXS and TEM, the blend composition was systematically correlated with the morphological and the mechanical properties in the lamellar phase. Elongation at break, toughness and Young's modulus were found to be substantially increased (e.g. $\varepsilon_{break} \approx 540\%$ for a 50 wt % blend) compared to the tapered diblock copolymer with its poor mechanical properties ($\varepsilon_{break} \approx 10\%$). The improved tensile properties with increased P(I-*co*-S)$_3$ content are explained by the bridging multiblock architecture, which is capable of connecting several vitrified PS-rich domains beyond entanglements (*i.e.* bridging conformation).

In the second part of the work the difference in domain spacings ($\Delta d$ by SAXS) of the tapered di- and multiblock copolymer constituents of the blends was systematically increased, giving rise to partially miscible and eventually to fully immiscible blends. In sharp contrast to miscible P(I-*co*-S)/P(I-*co*-S)$_n$ blends, an increasing degree of macrophase separation results in a decrease in both strain at break and toughness. This trend was explained based on the

SAXS/TEM findings, revealing the formation of macrophase-separated areas poor in P(I-*co*-S)$_n$ content. Such domains can be viewed as local defects, facilitating crack initialization, growth and ultimate failure of the materials. However, despite the poorer mechanical properties of the blends relative to the constituent P(I-*co*-S)$_n$ multiblock copolymers, their tensile properties exceed the strain at break and toughness of the corresponding tapered diblock copolymers by far.

Overall, our results demonstrate enhanced mechanical properties, particularly elastic response and toughness, introduced by the addition of a limited amount of a multiblock copolymer in diblock copolymers. These results may guide future industrial processes based on the synthesis of TPEs as blends of tapered diblock and multiblock copolymers with predictably mechanical properties.

## Supporting Information

Supporting Information is available from the Wiley Online Library or from the author.

## Acknowledgements

Philip Dreier and Tobias Johann are acknowledged for helpful discussions. We thank Jürgen Ludwig for specialty glassware and Monika Schmelzer for valuable support with SEC measurements. Andreas Hanewald and Dr. Kaloian Koynov are acknowledged for help with the mechanical characterization. M.G. and M.P. acknowledge the German Research Foundation (DFG GA 2169/7-1) for partial financial support of this work. The authors also thank the RMU Mainz-Darmstadt for funding.

## Conflict of Interest

The authors declare no conflict of interest.

Received: ((will be filled in by the editorial staff))
Revised: ((will be filled in by the editorial staff))
Published online: ((will be filled in by the editorial staff))

**References**


[1] N. Hadjichristidis, G. Floudas, S. Pispas, *Block copolymersSynthetic strategies, physical properties, and applications*, Wiley-Interscience, Hoboken, N.J. **2003**.

[2] a) A. H. Gabor, E. A. Lehner, G. Mao, L. A. Schneggenburger, C. K. Ober, *Chem. Mater.* **1994**, *6*, 927; b) H.-C. Kim, S.-M. Park, W. D. Hinsberg, *Chem. Rev.* **2010**, *110*, 146; c) C. Park, J. Yoon, E. L. Thomas, *Polymer.* **2003**, *44*, 6725; d) M. Appold, E. Grune, H. Frey, M. Gallei, *ACS Appl. Mater. Interfaces.* **2018**, *10*, 18202.

[3] K. Knoll, N. Nießner, *Macromol. Symp.* **1998**, *132*, 231.

[4] H. Geoffrey, R. Milkovich (Shell Oil Co) *U.S. Patent* 3,265,765, **1962**.

[5] J. G. Drobny, Ed., *Handbook of Thermoplastic Elastomers*, Elsevier. **2007**.

[6] M. Morton, "Mechanisms of Reinforcement of Elastomers by Polymeric Fillers", in *Multicomponent polymer systems.* American Chemical Society, Washington, DC. **1971**, p. 490 ff.

[7] A. Noshay, J. E. McGrath, *Block copolymers. Overview and critical survey*, 2nd edition, Acad. Pr, Orlando u.a. **1987**.

[8] a) N. Hadjichristidis, A. Hirao, Eds., *Anionic polymerization: Principles, practice, strength, consequences and applications*, Tokyo, Springer. **2015**; b) Z. Zhang, D. W. Grijpma, J. Feijen, *Macromol. Chem. Phys.* **2004**, *205*, 867; c) J. P. Bishop, R. A. Register, *Macromolecules.* **2010**, *43*, 4954.

[9] a) Y. Zhu, M. R. Radlauer, D. K. Schneiderman, M. S. P. Shaffer, M. A. Hillmyer, C. K. Williams, *Macromolecules.* **2018**, *51*, 2466; b) A. Touris, N. Hadjichristidis, *Macromolecules.* **2011**, *44*, 1969; c) M. T. Martello, D. K. Schneiderman, M. A. Hillmyer, *ACS Sustainable Chem. Eng.* **2014**, *2*, 2519.

[10] H. L. Hsieh, R. P. Quirk, *Anionic PolymerizationPrinciples and Practical Applications*, Dekker, New York. **1996**.

[11]G. Holden, E. T. Bishop, N. R. Legge, *J. Polym. Sci. C Polym. Symp.* **1969**, *26*, 37.

[12] F. S. Bates, M. A. Hillmyer, T. P. Lodge, C. M. Bates, K. T. Delaney, G. H. Fredrickson, *Science.* **2012**, *336*, 434.

[13] P. Georgopanos, U. A. Handge, C. Abetz, V. Abetz, *Polymer.* **2016**, *104*, 279.

[14] S. Förster, A. K. Khandpur, J. Zhao, F. S. Bates, I. W. Hamley, A. J. Ryan, W. Bras, *Macromolecules.* **1994**, *27*, 6922.

[15] N. Singh, M. S. Tureau, I. T. H.I.I. Epps, *Soft Matter.* **2009**, *5*, 4757.

[16] P. Hodrokoukes, G. Floudas, S. Pispas, N. Hadjichristidis, *Macromolecules.* **2001**, *34*, 650.

[17] M. Thunga, U. Staudinger, B. K. Satapathy, R. Weidisch, M. Abdel-Goad, A. Janke, K. Knoll, *J. Polym. Sci. B.* **2006**, *44*, 2776.

[18] M. Steube, T. Johann, E. Galanos, M. Appold, C. Rüttiger, M. Mezger, M. Gallei, A. H. E. Müller, G. Floudas, H. Frey, *Macromolecules.* **2018**, *51*, 10246.

[19] E. Galanos, E. Grune, C. Wahlen, A. H. E. Müller, M. Appold, M. Gallei, H. Frey, G. Floudas, *Macromolecules.* **2019**, *52*, 1577.

[20] S. D. Smith, R. J. Spontak, M. M. Satkowski, A. Ashraf, A. K. Heape, J. S. Lin, *Polymer.* **1994**, *35*, 4527.

[21] R. J. Spontak, S. D. Smith, *J. Polym. Sci. B.* **2001**, *39*, 947.

[22] a) S.-M. Mai, W. Mingvanish, S. C. Turner, C. Chaibundit, Fairclough, J. Patrick A., F. Heatley, M. W. Matsen, A. J. Ryan, C. Booth, *Macromolecules.* **2000**, *33*, 5124; b) L. Qiao, C. Leibig, S. F. Hahn, K. I. Winey, *Ind. Eng. Chem. Res.* **2006**, *45*, 5598.

[23] R. J. Spontak, J. J. Ryan, "Polymer blend compatibilization by the addition of block copolymers", in *Compatibilization of polymer blends.* Elsevier, Amsterdam. **2019**, p. 57 ff.

[24] a) N. Hadjichristidis, S. Pispas, G. Floudas, *Block Copolymers*, John Wiley & Sons, Inc, Hoboken, USA. **2002**; b) L. Leibler, *Macromolecules.* **1980**, *13*, 1602.

[25] G. Floudas, D. Vlassopoulos, M. Pitsikalis, N. Hadjichristidis, M. Stamm, *J. Chem. Phys.* **1996**, *104*, 2083.

[26] T. Hashimoto, K. Yamasaki, S. Koizumi, H. Hasegawa, *Macromolecules.* **1993**, *26*, 2895.

[27] T. Hashimoto, S. Koizumi, H. Hasegawa, *Macromolecules.* **1994**, *27*, 1562.

[28] L. Kane, M. M. Satkowski, S. D. Smith, R. J. Spontak, *Macromolecules.* **1996**, *29*, 8862.

[29] M. W. Matsen, *J. Chem. Phys.* **1995**, *103*, 3268.

[30] A. D. Vilesov, G. Floudas, T. Pakula, E. Y. Melenevskaya, T. M. Birshtein, Y. V. Lyatskaya, *Macromol. Chem. Phys.* **1994**, *195*, 2317.

[31] a) R. E. Cohen, N. W. Tschoegl, *International Journal of Polymeric Materials and Polymeric Biomaterials.* **1972**, *2*, 49; b) R. E. Cohen, N. W. Tschoegl, *International Journal of Polymeric Materials and Polymeric Biomaterials.* **1973**, *2*, 205.

[32] a) L. Kane, S. A. White, R. J. Spontak, *MRS Proc.* **1996**, *461*, 149; b) L. Kane, D. A. Norman, S. A. White, M. W. Matsen, M. M. Satkowski, S. D. Smith, R. J. Spontak, *Macromol. Rapid Commun.* **2001**, *22*, 281; c) J. Song, Y. Li, Q. Huang, T. Shi, L. An, *J. Chem. Phys.* **2007**, *127*, 94903.

[33] a) R. J. Spontak, J. M. Zielinski, G. G. Lipscomb, *Macromolecules.* **1992**, *25*, 6270; b) Smith, R. J. Spontak, Satkowski, Ashraf, Lin, *Physical review. B, Condensed matter.* **1993**, *47*, 14555.

[34] T. J. Hermel, S. F. Hahn, K. A. Chaffin, W. W. Gerberich, F. S. Bates, *Macromolecules.* **2003**, *36*, 2190.

[35] G. Fleury, F. S. Bates, *Macromolecules.* **2009**, *42*, 3598.

[36] Y. Mori, L. S. Lim, F. S. Bates, *Macromolecules.* **2003**, *36*, 9879.

[37] R. J. Spontak, S. D. Smith, A. Ashraf, *Macromolecules.* **1993**, *26*, 5118.

[38] J. H. Laurer, D. A. Hajduk, S. Dreckötter, S. D. Smith, R. J. Spontak, *Macromolecules.* **1998**, *31*, 7546.

[39] R. J. Spontak, J. C. Fung, M. B. Braunfeld, J. W. Sedat, D. A. Agard, A. Ashraf, S. D. Smith, *Macromolecules.* **1996**, *29*, 2850.

[40] T. Hashimoto, Y. Tsukahara, K. Tachi, H. Kawai, *Macromolecules.* **1983**, *16*, 648.

[41] R. Lach, R. Adhikari, R. Weidisch, T. A. Huy, G. H. Michler, W. Grellmann, K. Knoll, *J Mater Sci.* **2004**, *39*, 1283.

[42] R. Adhikari, M. Buschnakowski, W. Lebek, R. Godehardt, G. H. Michler, F. J. B. Calleja, K. Knoll, *Polym. Adv. Technol.* **2005**, *16*, 175.

[43] a) K. Karatasos, S. H. Anastasiadis, T. Pakula, H. Watanabe, *Macromolecules.* **2000**, *33*, 523; b) H. Watanabe, Y. Matsumiya, T. Sawada, T. Iwamoto, *Macromolecules.* **2007**, *40*, 6885;

[44] C. Livitsanou, M. Steube, T. Johann, H. Frey, G. Floudas, *Macromolecules.* **2020**, *53*, 3042.

[45] a) T. J. Hermel, L. Wu, S. F. Hahn, T. P. Lodge, F. S. Bates, *Macromolecules.* **2002**, *35*, 4685; b) M. E. Vigild, C. Chu, M. Sugiyama, K. A. Chaffin, F. S. Bates, *Macromolecules.* **2001**, *34*, 951.

[46] a) R. Adhikari, R. Lach, G.H. Michler, R. Weidisch, W. Grellmann, K. Knoll, *Polymer.* **2002**, *43*, 1943; b) C. Harrats, S. Thomas, G. Groeninckx, Eds., *Micro- and nanostructured multiphase polymer blend systems: phase morphology and interfaces*, Boca Raton, Fla., Taylor & Francis. **2006**.

[47] M. Steube, T. Johann, M. Plank, S. Tjaberings, A. H. Gröschel, M. Gallei, H. Frey, A. H. E. Müller, *Macromolecules.* **2019**, *52*, 9299.

**For Table of contents use only (size 55mm broad x 50 mm high)**

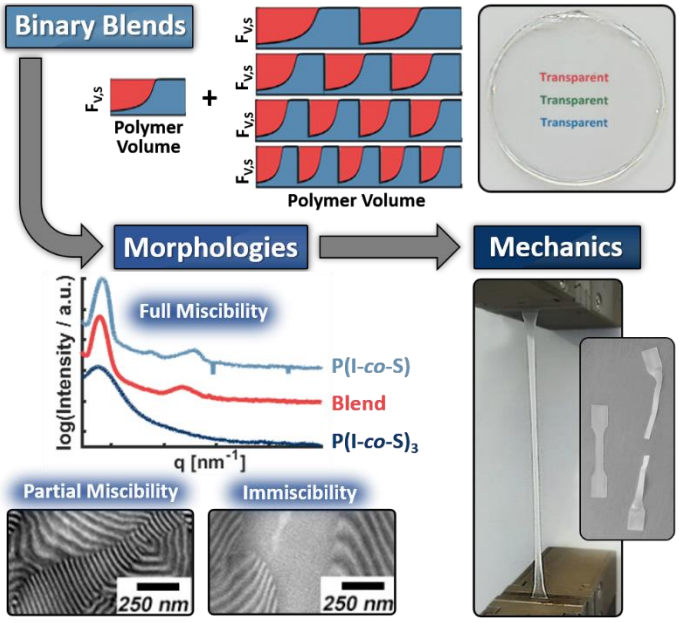

# Supporting Information

## Building Bridges by Blending: Morphology and Mechanical Properties of Binary Tapered Diblock/Multiblock Copolymer Blends

*Marvin Steube, Martina Plank, Markus Gallei, Holger Frey,* George Floudas**

**Table of Contents**

## 1. Materials, Experimental Procedures and Instrumentation

All chemicals and solvents were purchased from Acros Organics Co. and Sigma-Aldrich Co. Chloroform was used as received without further purification.
The synthesis and the characterization of the tapered di- and multiblock copolymers is described in a previous work.[1]

### *Polymer Characterization*

An in-depth characterization of the tapered block copolymers is given in a previous work.[1]

### *X-Ray Scattering*

Small-angle (SAXS) measurements were made using CuKα radiation (Rigaku Micro Max 007 x-ray generator, Osmic Confocal Max-Flux curved multilayer optics). 2D diffraction patterns were recorded on an Mar345 image plate detector at a sample-detector distance of 2060 mm. Intensity distributions as function of the modulus of the total scattering vector, $q = (4\pi/\lambda) \sin(2\theta/2)$, where $2\theta$ is the scattering angle, were obtained by radial averaging of the 2D datasets. Samples in the form of thick films (~1 mm) were prepared by slow solvent casting. Temperature-dependent measurements of 1 hour long were made by heating the films from 298 K to 503 K.

### *TEM Measurements*

For characterization of the tapered block copolymer morphology in the bulk state, the as prepared films were microtomed from surface to surface at -80 °C into thin slices of 30-50 nm thickness. The collected ultrathin sections were subsequently stained with osmium tetroxide ($OsO_4$) for selective staining of the PI domains, followed by investigation by TEM measurements.
Transmission electron microscopy (TEM) experiments were carried out using a Zeiss EM 10 electron microscope (Oberkochen, Germany) operating at 60 kV with a slow-scan CCD camera obtained from TRS (Tröndle, Morrenweis, Germany) in bright field mode. Camera was computer-aided using the Image SP software from TRS.

### *Tensile Tests*

Tensile tests were performed using a materials testing machine Z005 (Zwick/Roell, Germany). Tensile tests were carried out by exposing the stamped polymer dogbones to a uniaxial tension. Bone shape samples with thicknesses around 0.2 mm were drawn with rate of 10 mm/min at room temperatures. A Pre-Load of 0.1 N was applied with a Pre-Load speed of 5 mm/min. Dependencies of stress vs. draw ratio were recorded. Elastic modulus, elongation at break and stress at break were determined as averages of 8–15 independent drawing experiments performed at the same conditions. Transparent films were prepared with a thickness round 0.2 mm, obtained by slow evaporation from a chloroform solution followed a full removal of the solvent under reduced pressure and used for tensile tests without prior thermal annealing.

**2. Effect of the Tapered Multiblock Copolymer Content: AB/(AB)$_3$ Blends**

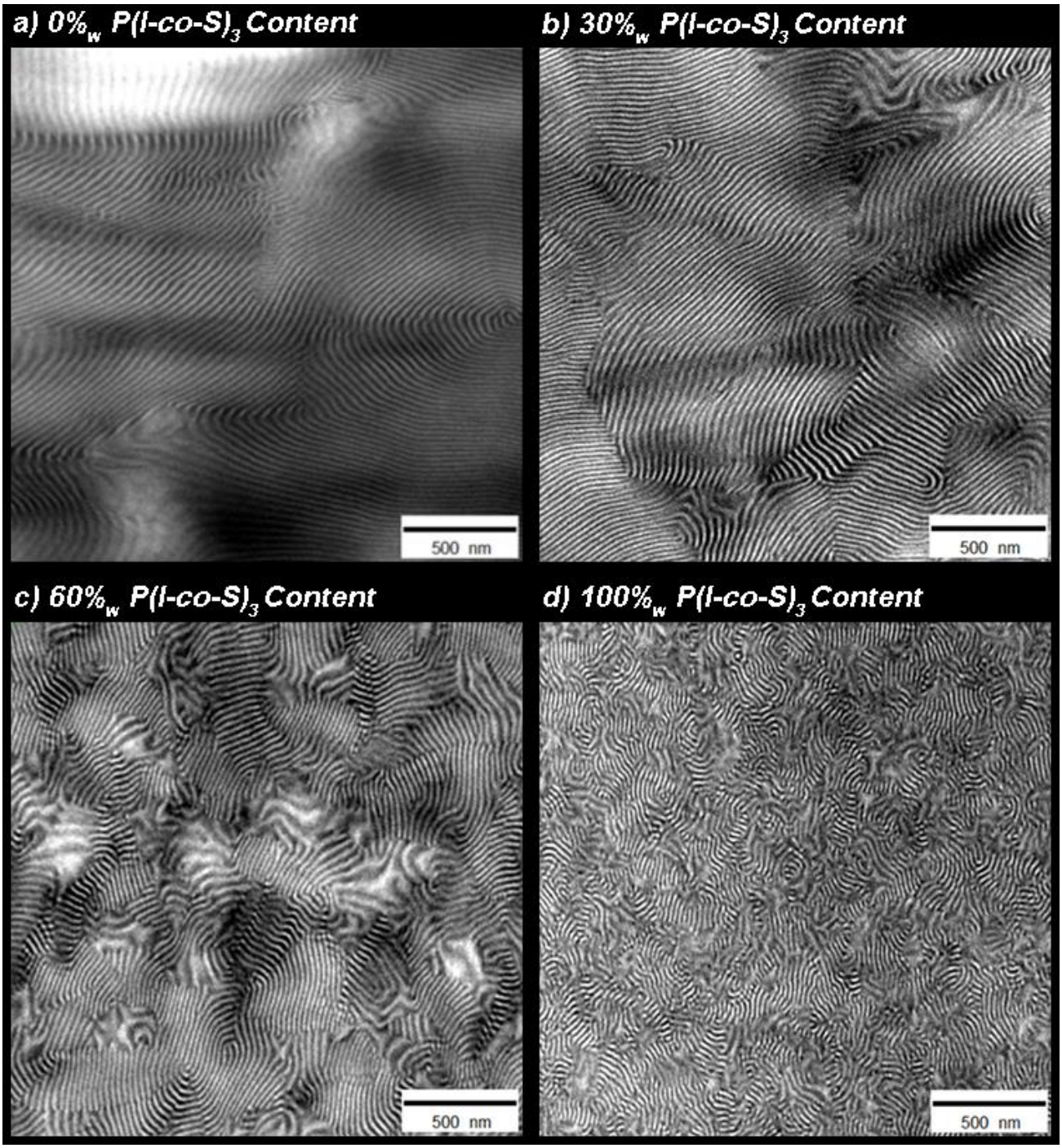


**Figure S1.** TEM images of P(I-*co*-S), P(I-*co*-S)/P(I-*co*-S)$_3$ blends and P(I-*co*-S)$_3$ (**Table 1**, Entry 1). The domain spacings in dependence of the P(I-*co*-S)$_3$ content are a) $d(0\%) = 30 \pm 3.2$ nm, b) $d(30\%) = 29 \pm 5.0$ nm, c) $d(60\%) = 26 \pm 3.2$ nm, d) $d(100\%) = 26 \pm 6.3$ nm, (**Table 2**, Entries 1, 5, 8 and 11), respectively. PI-rich phases are $OsO_4$-stained and appear electron opaque (dark).

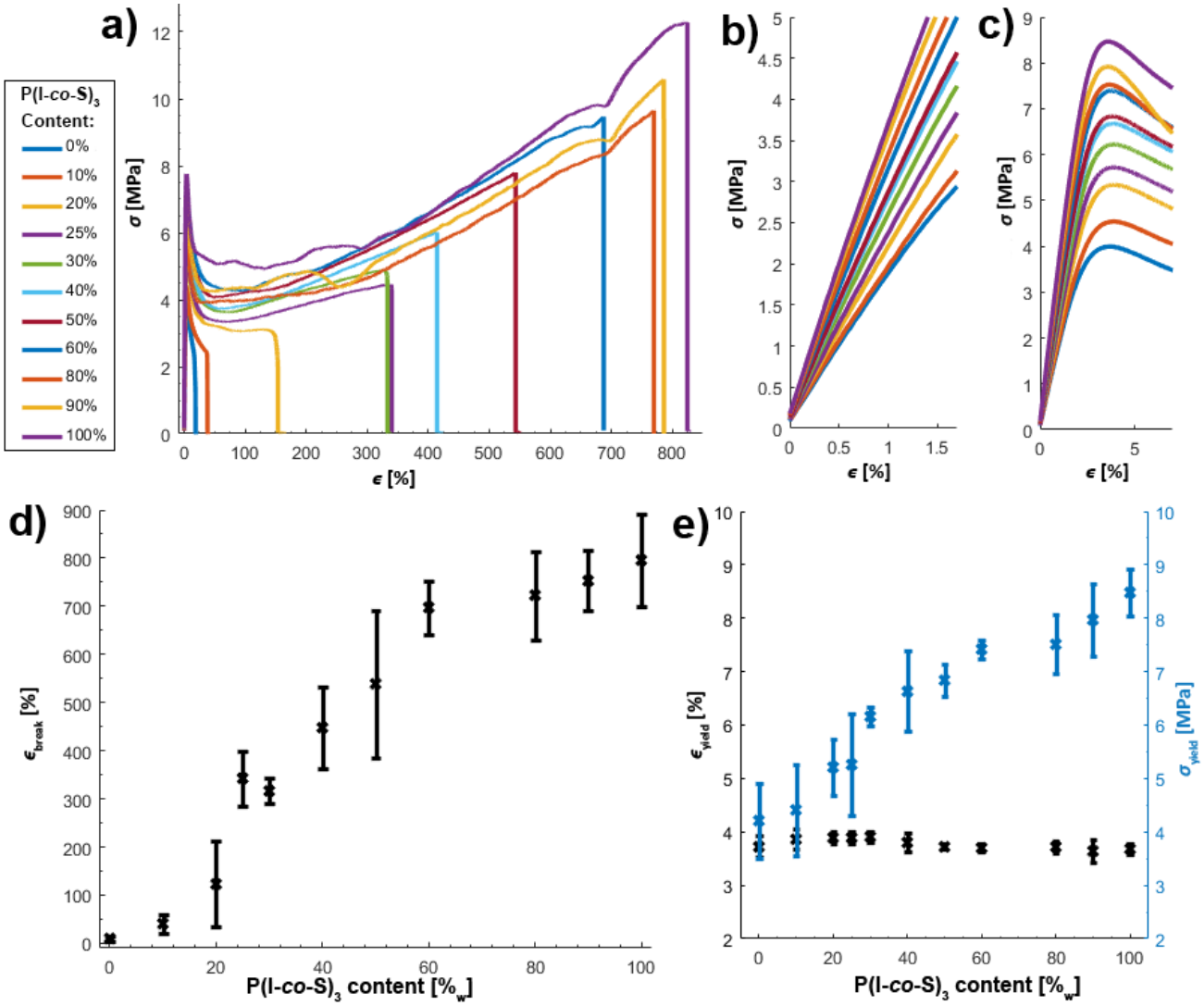


**Figure S2.** a) Representative stress-strain ($\sigma$-$\varepsilon$) diagrams for P(I-*co*-S), P(I-*co*-S)/P(I-*co*-S)$_3$ blends and P(I-*co*-S)$_3$ (Table 2). b) Linear elastic region ($\varepsilon \approx 0 - 1.5\%$), used to determine the Young's modulus. The elastic moduli ($E_{mod}$) were determined as the slope of first order fits. c) Visualization of the yield points, which were determined as the local maximum $\sigma_{yield}=\sigma_{max}(\varepsilon \approx 0 - 8\ \%)$ (**Figure S3b**). d) Strain at break ($\varepsilon_{break}$) as a function of the P(I-*co*-S)$_3$ content. e) Yield strain ($\varepsilon_{yield}$) and yield stress ($\sigma_{yield}$) as a function of the P(I-*co*-S)$_3$ content.

In contrast to the $\varepsilon_{break}$ (**Figure S2d**), the toughness shows a comparably large increase for P(I-*co*-S)$_3$ contents > 60%. explained by large values of $\sigma(\varepsilon)$ near $\varepsilon_{break}$.

Yield points are also a function of the P(I-*co*-S)$_3$ content (**Figure S2e**). While the yield stress ($\sigma_{yield}$) correlates with the P(I-*co*-S)$_3$ content, the yield strain does not show significant changes ($\varepsilon_{yield}$ = 3.8 % ± 0.1). The increase in $\sigma_{yield}$ can be explained by an increasing force required to break the glassy PS domains.[2] Similar effects are observed by Spontak *et al.* and ascribed to an increased architecture-enhanced microstructural interconnectivity (i.e. number of bridges).[3] In this work, this effect is probably also a function of the glass transition temperature of the PS-rich phase, showing comparably larger values for P(I-*co*-S)$_3$ ($T_{g,PS\text{-}rich} \approx 90$ °C) compared to P(I-*co*-S)$_1$ ($T_{g,PS\text{-}rich} \approx 80$ °C).[1]

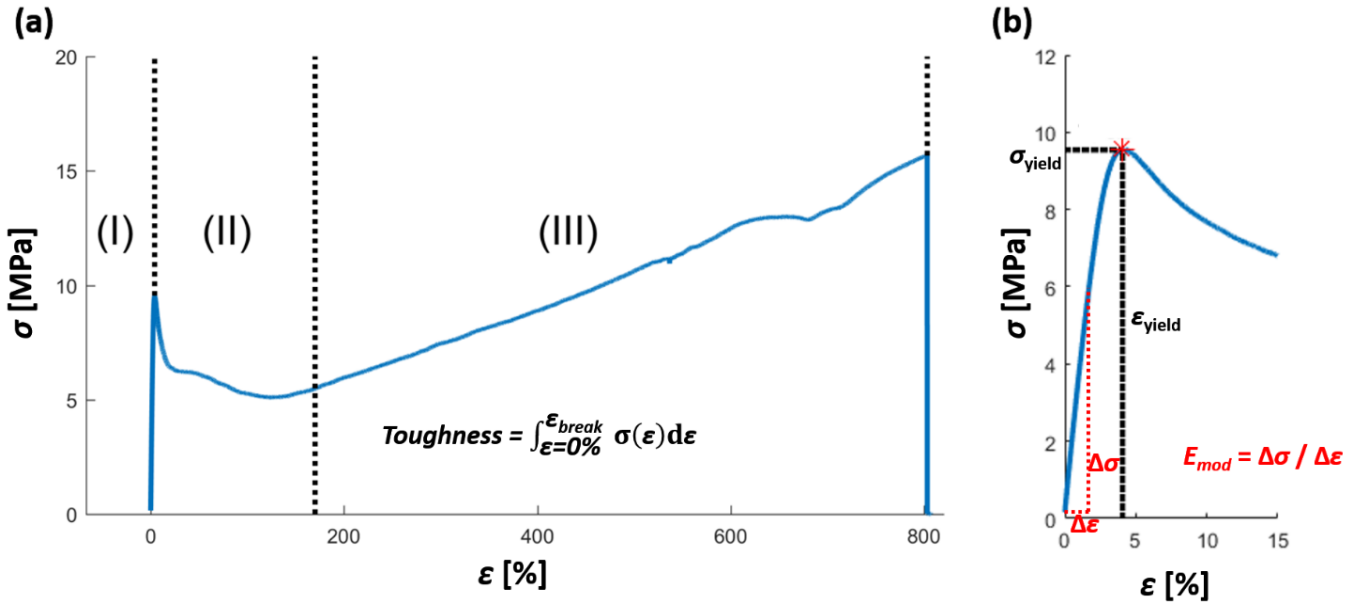


**Figure S3.** a) A typical stress-strain diagram, which is obtained for the multiblock copolymers investigated in this work. (I) Elastic regime, (II) Necking regime, (III). Strain-hardening regime. Stretching the sample in regime (I), leads to a reversible recovery of the material. Further stretching of the sample (regime II and III) also leads to irreversible viscous flow and only partial recovery of the material. The toughness is obtained by numeric integration of $\sigma(\varepsilon)$. b) The yield point is obtained as the local maximum at low strains. The elastic modulus is determined as the slope of the first order fit in the linear region of $\sigma(\varepsilon)$.

### 3. Effect of the Tapered Multiblock Copolymer Content: AB/(AB)3 Blends

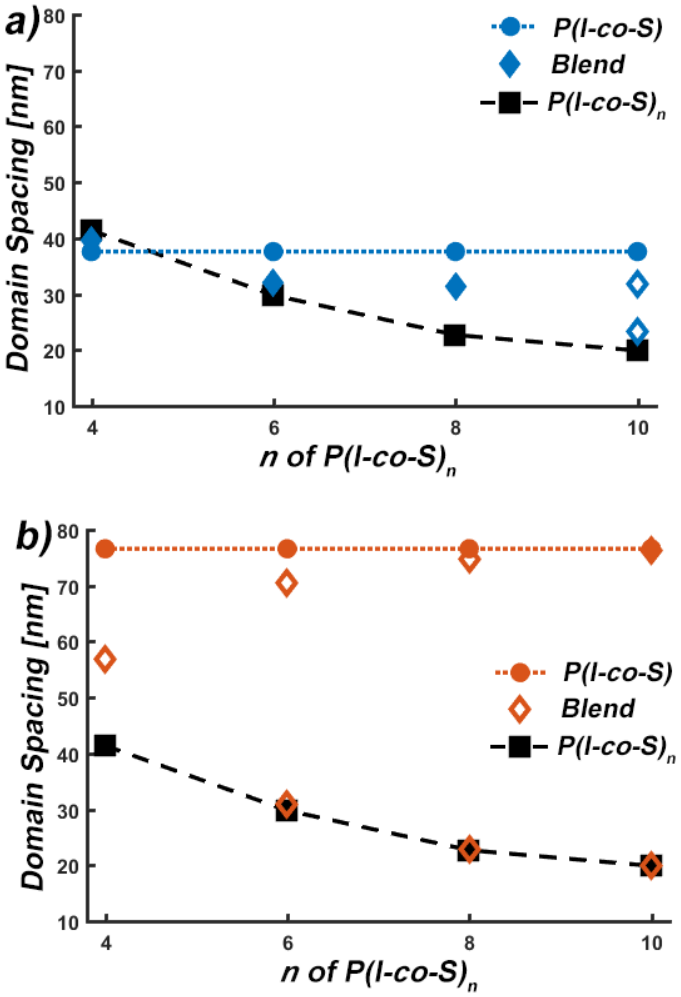


**Figure S4.** Overview of domain sizes observed in scattering results. Blend series with a) $d_{P(I\text{-}co\text{-}S)}$ = 38 nm leading to $\Delta d$ = -4 – 18 nm (**Table 3** Entry 2) and b) $d_{P(I\text{-}co\text{-}S)}$ = 77 nm leading to $\Delta d$ = 35 – 57 nm (**Table 3** Entry 3) are given. The domain sizes of the respective P(I-*co*-S) copolymer are visualized as a colored, dotted line in both plots. The domain sizes of the P(I-*co*-S)*n* copoylmers are visualized as black squares as a function of *n*. Points of the P(I-*co*-S) and P(I-*co*-S)$_n$ copolymer are interconnected by lines to guide the eye. Blend samples are visualized as diamonds; open symbols indicate macrophase separation.

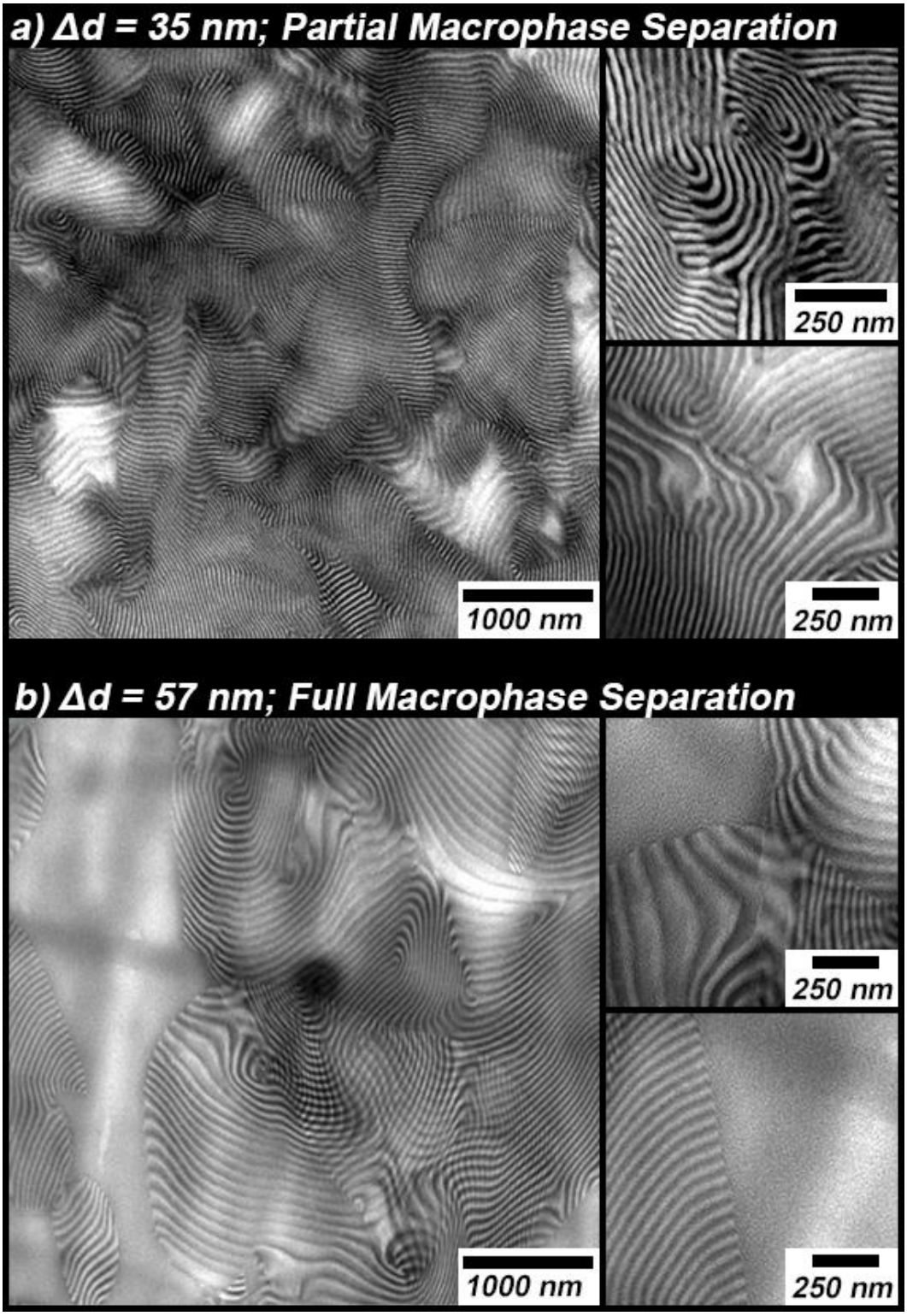


**Figure S5.** TEM measurements of a a) partial macrophase separated P(I-*co*-S)/P(I-*co*-S)$_2$ blend (**Table 1** Entry 3.1) and a b) full macrophase separated P(I-*co*-S)/P(I-*co*-S)$_5$ blend (**Table 1** Entry 3.4) with domain spacings of a) *d*(P(I-*co*-S)) = 41 ± 3.2 nm; *d*(P(I-*co*-S)$_2$) = 34 ± 2.1 and b) *d*(P(I-*co*-S)) = 58 ± 18 nm; *d*(P(I-*co*-S)$_5$) = n.d. as obtained by TEM imaging. PI-rich phases are $OsO_4$-stained and appear electron opaque (dark).

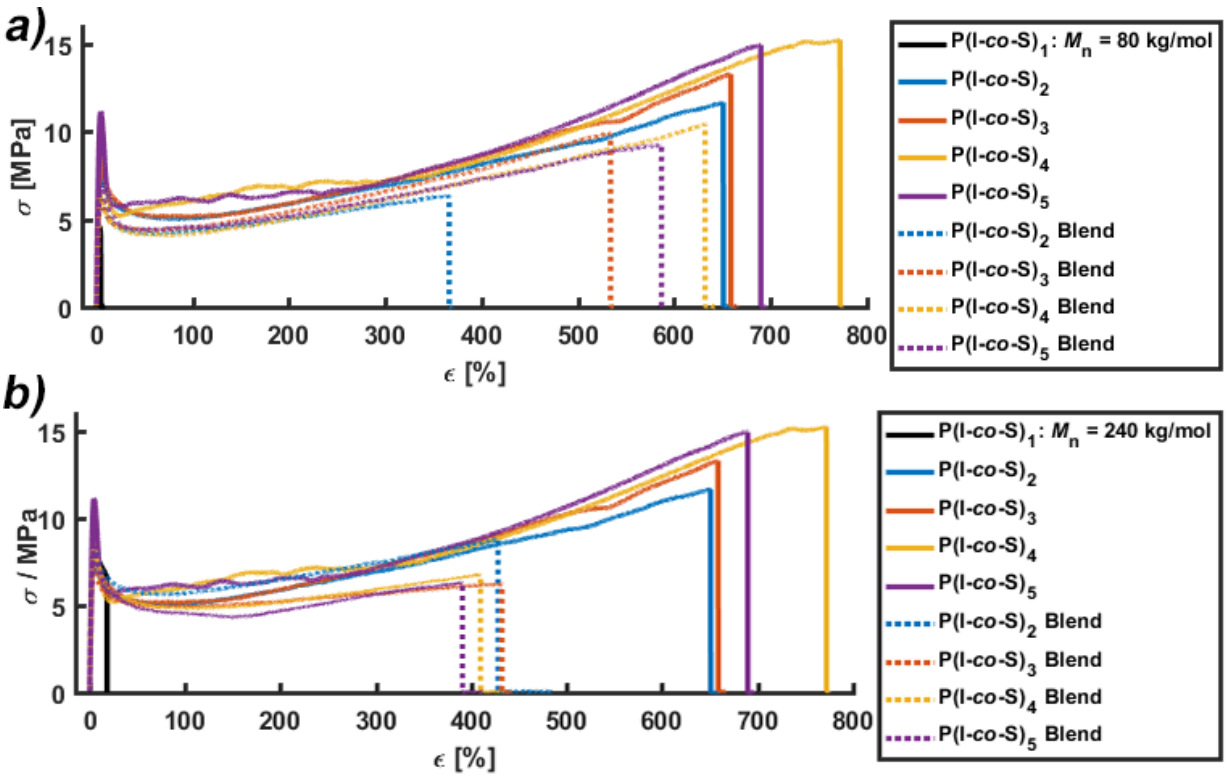


**Figure S6.** Representative stress-strain ($\sigma$-$\varepsilon$) diagrams for two P(I-*co*-S)/P(I-*co*-S)$_n$ blending series with diverging domain sizes for $n$=2-5. a) $\Delta d$=-4 to 18 nm (**Table 1;** Entry 2); b) $\Delta d$=36 to 57 nm (**Table 1;** Entry 3).

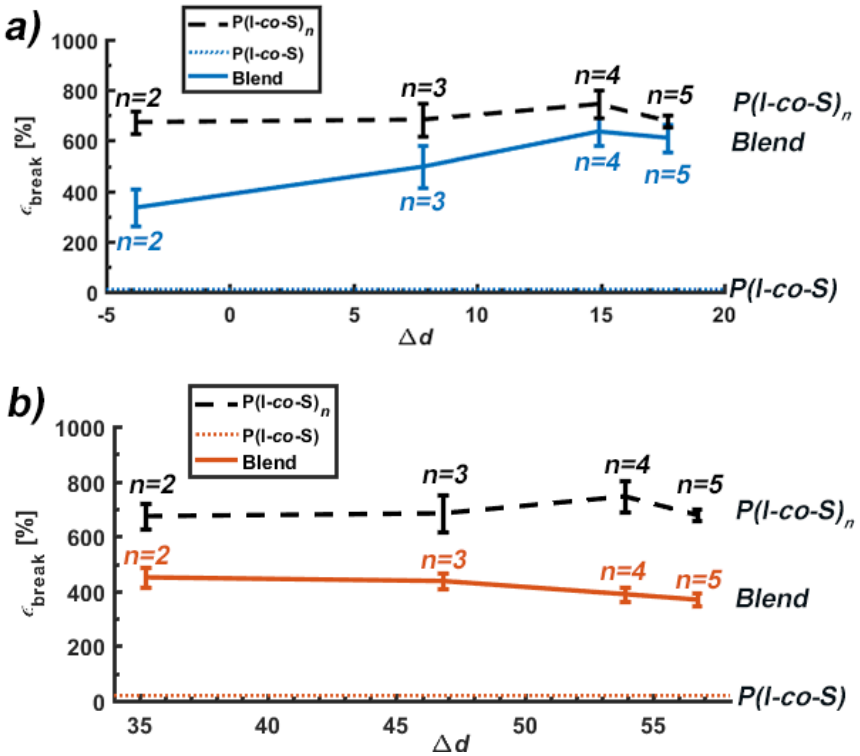


**Figure S7.** The strain at break of P(I-*co*-S) (dashed line), P(I-*co*-S)$_n$ (dotted line) and the respective blendblends (straight line) as a function of $\Delta d$. a) blending series with $\Delta d$ = -4- 18 nm (blue; **Table 1** Entry 2 and **Figure 6** left), b) $\Delta d$ = 35-57 nm (red; **Table 1** Entry 3 and **Figure 6** right). The values are interpolated as a guideline for the eye.

**Table S1.** Mechanical data of P(I-*co*-S) and P(I-*co*-S)$_n$ copolymers (*cf.* **Table 1**) determined via tensile testing. Errors are given as the standard deviation ($\sigma$ interval) from 8-15 independent drawing experiments.

| Entry | Tapered Copolymer | $M_{n,target}$ [kg/mol] | $\varepsilon_{break}$ [%] | Toughness [J/m$^3$] | $T_{g,PI\text{-}rich}$ a) | $T_{g,PS\text{-}rich}$ a) |
|---|---|---|---|---|---|---|
| 1 | P(I-*co*-S) | 80 | 10±5.0 | 0.33±0.15 | -37±12 | 80±11 |
| 2 | P(I-*co*-S) | 240 | 19±1.8 | 1.4±0.12 | -40±8 | 102±8 |
| 3.1 | P(I-*co*-S)$_2$ | 240 | 670±45 | 51±7.4 | -40±4 | 99±12 |
| 3.2 | P(I-*co*-S)$_3$ | 240 | 680±65 | 55±9.9 | -37±6 | 91±18 |
| 3.3 | P(I-*co*-S)$_4$ | 240 | 750±56 | 65±7.8 | -36±6 | 82±16 |
| 3.4 | P(I-*co*-S)$_5$ | 240 | 680±22 | 57±5.2 | -33±8 | 74±15 |
| 4 | P(I-co-S)$_3$ | 400 | 800±96 | 61±12 | -38±6 | 98±13 |

a) The first derivative of the heat flow is given in a previous work.[1]

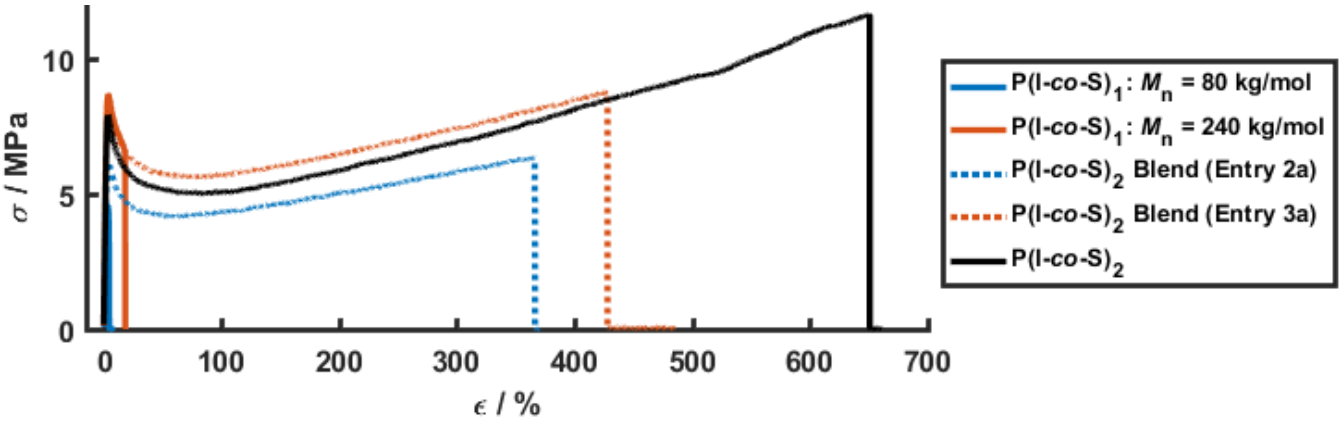


**Figure S8.** Representative stress-strain ($\sigma$-$\varepsilon$) diagrams for two P(I-*co*-S)/P(I-*co*-S)$_2$ blends (**Table 1** Entry 2.1 and 3.1) as well as the respective P(I-*co*-S) and P(I-*co*-S)$_2$ copolymers.

## References

[1] M. Steube, T. Johann, E. Galanos, M. Appold, C. Rüttiger, M. Mezger, M. Gallei, A. H. E. Müller, G. Floudas, H. Frey, *Macromolecules.* **2018**, *51*, 10246.
[2] D. Long, P. Sotta, *Rheol Acta.* **2007**, *46*, 1029.
[3] S. D. Smith, R. J. Spontak, M. M. Satkowski, A. Ashraf, A. K. Heape, J. S. Lin, *Polymer.* **1994**, *35*, 4527.